

Technical Report Documentation Page

1. Report No. FHWA/TX-09/0-5445-3		2. Government Accession No.		3. Recipient's Catalog No.	
4. Title and Subtitle Evaluation of MEPDG with TxDOT Rigid Pavement Database			5. Report Date July 2009		
			6. Performing Organization Code		
7. Author(s) Moon Won			8. Performing Organization Report No. 0-5445-3		
9. Performing Organization Name and Address Center for Transportation Research The University of Texas at Austin 3208 Red River, Suite 200 Austin, TX 78705-2650			10. Work Unit No. (TRAIS)		
			11. Contract or Grant No. 0-5445		
12. Sponsoring Agency Name and Address Texas Department of Transportation Research and Technology Implementation Office P.O. Box 5080 Austin, TX 78763-5080			13. Type of Report and Period Covered Technical Report 9/1/2005 – 8/1/2008		
			14. Sponsoring Agency Code		
15. Supplementary Notes Project performed in cooperation with the Texas Department of Transportation and the Federal Highway Administration.					
16. Abstract <p>TxDOT initiated the rigid pavement database project to collect information on the general performance of portland cement concrete (PCC) pavement as well as to collect project-level information on PCC pavement responses and performance. A total 27 sections were selected statewide and detailed information was collected such as load transfer efficiency at small, medium, and large crack spacing and for two different seasons: summer and winter. Also collected were crack spacing information and slab deflections. Efforts were made to calibrate the punchout model in MEPDG. Review of the punchout model in MEPDG revealed that it is quite sophisticated, with a number of variables involved. It assumes that longitudinal cracking is induced by top-down cracking. The model is more applicable to CRCP with an asphalt shoulder. On the other hand, the model might not be appropriate for the punchout analysis of CRCP with tied-concrete shoulder. Sensitivity analyses were conducted to investigate the effects of selected input variables on punchouts. Zero-stress temperature (ZST) had quite a large effect, because crack width and LTE depend to a large extent on ZST. The MEPDG equation for crack width tends to over-predict crack width and appropriate calibration constant needs to be determined. The comparison of actual punchout with a predicted value from MEPDG using national calibration constants shows a marked difference. MEPDG over-predicted punchout more than 30 times. When the calibration constant for crack width was reduced from 1 to 0.5, the predicted punchout became more reasonable.</p> <p>It appears that many distresses identified and recorded as punchouts in Texas are not actually punchouts caused by structural deficiency. Rather, most of them are due to imperfections in design details and/or construction/materials quality issues. Horizontal cracking appears to be the major cause of distresses in CRCP in Texas. The interactions between longitudinal steel and concrete in response to dynamic wheel loading applications appear to be the cause of horizontal cracking. Efforts should be made to accurately identify punchout during field evaluations. At this point, the punchout information in TxDOT's PMIS doesn't appear to be accurate.</p> <p>Manual for administrator of the database developed in this study is contained in this report.</p>					
17. Key Words cracking, CRCP, punchout, MEPDG			18. Distribution Statement No restrictions. This document is available to the public through the National Technical Information Service, Springfield, Virginia 22161; www.ntis.gov.		
19. Security Classif. (of report) Unclassified		20. Security Classif. (of this page) Unclassified		21. No. of pages 68	
22. Price					



Evaluation of MEPDG with TxDOT Rigid Pavement Database

Moon Won

CTR Technical Report:	0-5445-3
Report Date:	July 2009
Project:	0-5445
Project Title:	Project Level Performance Database for Rigid Pavements in Texas
Sponsoring Agency:	Texas Department of Transportation
Performing Agency:	Center for Transportation Research at The University of Texas at Austin

Project performed in cooperation with the Texas Department of Transportation and the Federal Highway Administration.

Center for Transportation Research
The University of Texas at Austin
3208 Red River
Austin, TX 78705

www.utexas.edu/research/ctr

Copyright (c) 2009
Center for Transportation Research
The University of Texas at Austin

All rights reserved
Printed in the United States of America

Disclaimers

Author's Disclaimer: The contents of this report reflect the views of the authors, who are responsible for the facts and the accuracy of the data presented herein. The contents do not necessarily reflect the official view or policies of the Federal Highway Administration or the Texas Department of Transportation (TxDOT). This report does not constitute a standard, specification, or regulation.

Patent Disclaimer: There was no invention or discovery conceived or first actually reduced to practice in the course of or under this contract, including any art, method, process, machine manufacture, design or composition of matter, or any new useful improvement thereof, or any variety of plant, which is or may be patentable under the patent laws of the United States of America or any foreign country.

Engineering Disclaimer

NOT INTENDED FOR CONSTRUCTION, BIDDING, OR PERMIT PURPOSES.

Project Engineer: Moon Won
Professional Engineer License State and Number: Texas No. 76918
P. E. Designation: Research Supervisor

Acknowledgments

The author expresses his appreciation to the project director, Ms. Hua Chen, and the program coordinator, Mr. Charles Gaskin. Valuable comments were received from the Project Monitoring Committee (PMC) members, Ms. Lisa Lukefahr, and Dr. German Claros. Their contributions are appreciated. Thanks to the district pavement engineers who provided unconditional support during field evaluation and FWD testing, and Adam Finley for his invaluable support in field testing. Sureel Saraf with the assistance of Professor Kevin Mulligan at Texas Tech University developed the rigid pavement database and their effort is greatly appreciated.

Table of Contents

Chapter 1. Introduction.....	1
1.1 Scope of the Report.....	2
Chapter 2. Review of MEPDG Punchout Model	3
2.1 Punchout Development Mechanisms in MEPDG	3
2.2 Relationship among Variables in Punchout Development Model in MEPDG.....	4
2.3 Sensitivity Analysis	6
2.3.1 Effect of Zero-Stress Temperature on CRCP Behavior and Punchout.....	6
2.3.2 Effect of Built-in Curling on CRCP Behavior and Punchout	12
2.3.3 Effect of Slab Thickness and Steel Percentage on CRCP Behavior and Punchout	12
2.4 Discussion.....	15
Chapter 3. Calibration of Punchout Model.....	21
3.1 Information Collected for the Calibration of Punchout Model.....	21
3.2 US 287 Section in Wichita Falls District.....	22
3.3 MEPDG Evaluation of this Section	25
3.4 Discussion.....	27
Chapter 4. Punchout Mechanism in CRCP in Texas	31
4.1 Distresses in CRCP in Texas	31
4.1.1 Distresses due to Horizontal Cracking.....	32
4.1.2 Distresses due to Horizontal Cracking.....	32
4.1.3 Fatigue Cracking	39
4.1.4 Other Distress Types.....	41
4.2 Discussion.....	43
Chapter 5. Manual for Database Administrator	45
5.1 RPDB Contents.....	45
5.1.1 General Pavement Section Information	45
5.1.2 Detailed Pavement Section Testing Data.....	45
5.1.3 On-site Pictorial Presentation for Each Test Section.....	46
5.2 Internal Structure of RPDB.....	46
5.3 Development of the Web-Application.....	47
5.3.1 Developing the Map Document	48
5.3.2 Authoring and Publishing a Map Service using ArcGIS Server Manager	49
Chapter 6. Summary and Recommendations	53
References.....	55

List of Figures

Figure 2.1: Mechanism of punchout development (1).....	3
Figure 2.2: Effect of ZST on crack width and LTE.....	5
Figure 2.3: Effect of ZST and LTE on punchout.....	5
Figure 2.4: ZST effects	6
Figure 2.5: Measured ZST	7
Figure 2.6: Variations in temperature of concrete placed at different times of day	8
Figure 2.7: Steel strain measurements and variations.....	10
Figure 2.8: Crack data.....	10
Figure 2.9: Shrinkage and crack widths.....	11
Figure 2.10: Effect of built-in curling on punchouts	12
Figure 2.11: Effects on punchouts	13
Figure 2.12: Core and spalling.....	16
Figure 2.13: Effect of transverse crack stiffness on LTE	18
Figure 2.14: Variations of LTE up to punchout development	19
Figure 3.1: Condition of US 287	24
Figure 3.2: Effect of construction month.....	26
Figure 3.3: Sensitivity of calibration constants on punchout.....	28
Figure 3.4: Effect of calibration constants	29
Figure 4.1: Examples of punchout in TxDOT PMIS Rater’s Manual	32
Figure 4.2: Punchout and horizontal cracking	32
Figure 4.3: Distresses observed	33
Figure 4.4: Distress at coring locations.....	33
Figure 4.5: Condition of cores taken.....	34
Figure 4.6: Longitudinal cracking and sample core.....	35
Figure 4.7: Distresses in US 281	36
Figure 4.8: Longitudinal and horizontal cracks	37
Figure 4.9: Longitudinal cracking on steel	38
Figure 4.10: Fine longitudinal cracks	38
Figure 4.11: Transverse fatigue crack formed between two old transverse cracks	40
Figure 4.12: Transverse fatigue crack.....	41
Figure 4.13: Surface distress.....	42
Figure 4.14: Distress at perimeter and joint.....	42
Figure 5.1: RPDB internal structure diagram	47
Figure 5.2: Map Document	48
Figure 5.3: Attributes of Pavement Sections	49

Figure 5.4: Logging in to ArcGIS Server Manager	50
Figure 5.5: Adding the Map Document to the Web-Service	50
Figure 5.6: Selecting and Adding Tasks to the Map Service.....	51
Figure 5.7: Adding Map Elements to the Map Service	52

List of Tables

Table 3.1: General description of Wichita Falls Test Section	23
Table 3.2: LTE evaluation at cracks with various spacing	25

Chapter 1. Introduction

Structural responses of continuously reinforced concrete pavement (CRCP) are quite complicated, because there are a number of variables affecting the structural behavior and the interactions among the variables are complex. It becomes quite difficult to identify and quantify the effects of the variables on long-term performance of CRCP because CRCP distresses take quite a long time to develop. One of the best ways to investigate CRCP behavior and long-term performance is to conduct periodic detailed evaluations of CRCP behavior on selected sections. The findings from such efforts could be quite valuable in that they can be used to evaluate the effectiveness of the specific CRCP system, which includes design, materials, and construction methods employed, and they also can be used to calibrate any mechanistic-based CRCP design procedures. This project was initiated with the objectives of achieving those two goals: evaluate the performance of CRCP in general in Texas and gather in-depth quality data that could be used to calibrate any mechanistic-based CRCP design procedures.

In general, CRCP performance has been satisfactory in Texas. Most of the distresses observed in quite old CRCP sections, more than 30 years old, were due to inadequate structural designs, which include the use of non-stabilized subbase, asphalt shoulder, and to a lesser degree, insufficient slab thickness. However, it should be recognized that those sections provided design lives much longer and more traffic than intended. The primary distress type in those sections is similar to edge punchout. To address those distress problems and to improve overall portland cement concrete (PCC) pavement performance, the Texas Department of Transportation (TxDOT) made three changes in 1980s: (1) the use of stabilized subbase, either 4-in. thick asphalt layer or 6-in. cement stabilized subbase with 1-in. hot mix asphalt on top, (2) the use of tied-concrete shoulder, and (3) the use of thicker slabs by using higher reliability in the 1986 AASHTO design procedures. These three changes improved CRCP performance substantially and thus punchouts meeting the traditional definition are quite rare in CRCP sections built with these three changes incorporated.

In order to improve the accuracy of pavement design procedures, national efforts were made in the late 1990s and the most advanced pavement design program, called MEPDG (mechanistic-empirical pavement design guide), was developed under NCHRP (National Cooperative Highway Research Program) 1-37(A) (1). This design procedure incorporated the most current state of knowledge in structural and materials behavior in response to environmental loading (temperature and moisture variations) as well as traffic loading, and used efficient methods to expedite the numerical computations. MEPDG is user-friendly, even though it requires many more input variables than the 1993 AASHTO Pavement Design Guide (2). The CRCP module in the MEPDG was calibrated using CRCP performance data collected nationwide and the results could very well be suitable for use in Texas. However, the environmental condition as well as the pavement design features used in Texas, such as the depth of longitudinal steel, might be different from the rest of the country. Calibrating MEPDG using the data from CRCP sections in Texas might result in more accurate pavement design program. As stated earlier, collecting the information needed for the calibration of MEPDG was one of the primary objectives of this study.

1.1 Scope of the Report

This report describes the efforts made to calibrate the punchout model in MEPDG using information obtained in this project and the development of rigid pavement database (RPDB).

Chapter 2 reviews the punchout model adopted in MEPDG. Sensitivity analyses were conducted to evaluate the effects of selected variables on punchouts and other structural responses. In-depth discussions are provided regarding the validity of the assumptions made in the punchout model in MEPDG.

Chapter 3 describes the effort to compare punchout information from a section on US 287 in the Wichita Falls District that is more than 38 years old with the predicted punchout from MEPDG. Because MEPDG requires extensive input information, some of which is not known for the old section under investigation, actual crack spacing was compared with predicted and best estimate was made for certain input values.

Chapter 4 discusses distress types observed in CRCP in Texas, along with possible mechanisms. It appears that a majority of distresses identified and recorded as punchouts may not be actual punchouts. Rather, they could be due to design deficiencies and/or construction/materials quality issues. In other words, a majority of distresses identified as punchouts are not due to structural deficiency. This finding is quite significant from a standpoint of its effect on CRCP design. Its implications are discussed.

Chapter 5 contains manual for administrator of rigid pavement database. Web-based and GIS-based rigid pavement database was developed in this study and this chapter discusses how to manage the database for administrator.

Chapter 6 presents the summary and recommendations.

Chapter 2. Review of MEPDG Punchout Model

In CRCP, full-depth punchout is the only structural distress and is one of the two performance indicators in MEPDG. The other performance indicator is the ride in terms of IRI (international roughness index). Punchout is the distress manifested by the slab segment surrounded by two closely spaced transverse cracks and a longitudinal crack, with the slab segment being somewhat pushed down by the repeated applications of truck traffic. Punchout represents serious distress, because it degrades ride quality and could pose danger to the traveling public. It is important that CRCP be designed properly to minimize or prevent punchout distress within design life. This chapter describes the punchout mechanisms adopted in the MEPDG along with the information needed for the calibration of the punchout model.

2.1 Punchout Development Mechanisms in MEPDG

Punchout development mechanisms adopted in MEPDG, to be referred to “punchout model” in this report, are quite complicated and well described in Appendix LL of the NCHRP 1-37(A) (I). Detailed description is not provided in this report; rather, a brief review is presented, along with in-depth discussion where needed. Figure 2.1 illustrates the punchout development mechanism adopted in MEPDG.

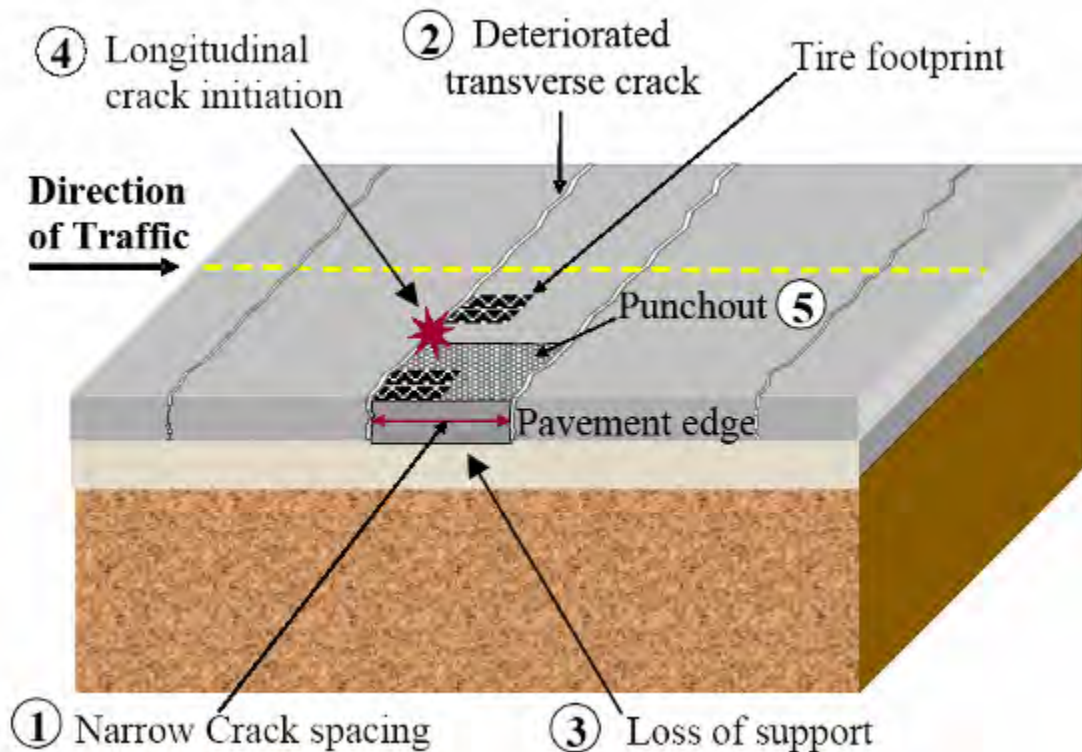


Figure 2.1: Mechanism of punchout development (1)

The mechanism can be explained as follows:

1. A slab segment with narrow transverse crack spacing (2 ft or less) exists.
2. Large transverse crack widths and repeated heavy loads degrade load transfer efficiency (LTE) across transverse cracks.
3. Loss of support takes place along the pavement edge due to subbase erosion.
4. Drying shrinkage at the top of the slab and negative temperature gradients through the slab depth further magnify bending stress in the transverse direction at 4 ft away from the pavement edge.
5. Passages of heavy axles causing repetitive cycles of excessive tensile bending stresses lead to top-down longitudinal fatigue cracking that defines punchout.

It is important to understand that this mechanism is more appropriate for CRCP with asphalt shoulder, because it is assumed that the critical transverse stress is at the top of the slab, with 4 ft from pavement edge. If tied-concrete shoulder is used, the critical transverse stress will be at the bottom of the slab, causing bottom-up longitudinal cracking, and the application of this model would be inappropriate.

2.2 Relationship among Variables in Punchout Development Model in MEPDG

The mechanism discussed illustrates that the degradation of LTE, along with an increase in crack width and loss of support in the subbase, plays a major role in the punchout model. In this model, large crack width and loss of support are the causes of low LTE, which facilitates the development of punchout. Estimating loss of support is quite complicated, and until now, the loss of support has not been a direct pavement design input consideration, except for including its effect on the reduction of modulus of subgrade reaction. In the punchout model, however, loss of support is a direct consideration for punchout development as will be discussed later. In short, a fixed value of LTE considering loss of potential is assigned to each subbase type. Accordingly, for a subbase type considered in the pavement design, LTE becomes a function of crack width, with a minor effect exerted by longitudinal reinforcement. It is important to evaluate the correlation between crack width and LTE. Preliminary sensitivity analysis conducted on MEPDG by the research team indicated a strong correlation between zero-stress temperature and transverse crack width as shown in Figure 2.2-(a). The input values for all the MEPDG analyses presented in this chapter were obtained from the test section in the database project, Section 3US287-1 in the Wichita Falls District, except for the values noted. Figure 2.2-(a) compares predicted crack widths of the sections built in two different zero-stress temperatures (ZST); one is at 80 F and the other at 100 F. It is observed that crack width changes with time, and also fluctuates within a year following seasonal temperature variations. The section built at 100 F ZST has greater crack widths than those built at 80 F ZST. Figure 2.2-(b) shows the variations in LTE of the two sections. The section with 100 F ZST experiences more rapid decrease in LTE than the section with 80 F ZST. It follows that larger crack widths with 100 F ZST shown in Figure 2.2-(a) resulted in lower LTE compared with those at 80 F ZST.

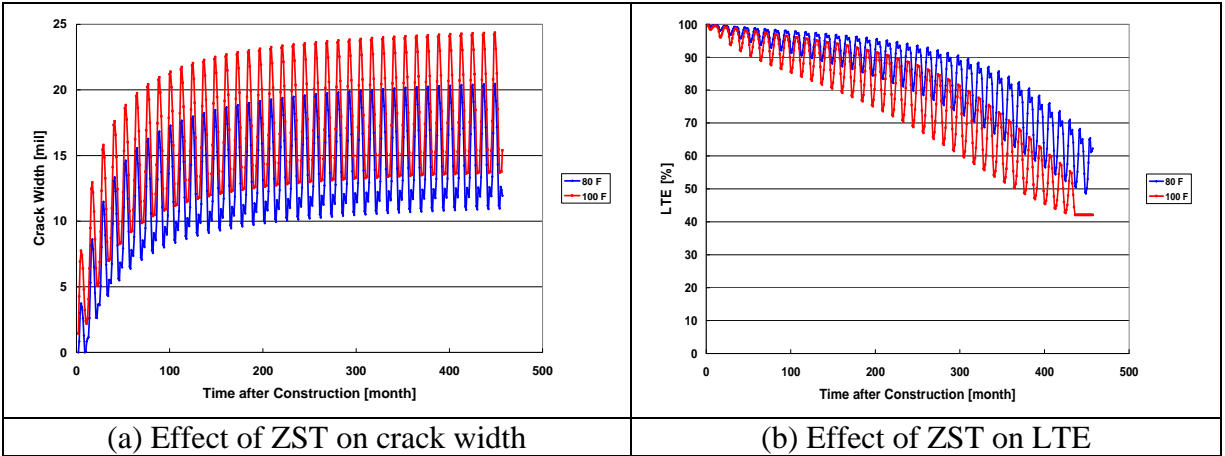


Figure 2.2: Effect of ZST on crack width and LTE

The effect of ZST on punchout is shown in Figure 2.3-(a). It is observed that the number of punchouts in the section constructed at 100 F ZST was almost double of the number of the section with 80 F ZST. Larger crack width and resulting lower LTE in the section built with 100 F ZST are responsible for this large increase in punchouts compared with the section built with 80 F ZST. This result indicates high sensitivity of the punchout predictions of MEPDG to ZST, which has significant implications in pavement design as will be discussed later in this chapter. To further investigate the effect of LTE on punchout, various LTE values were generated by using different longitudinal steel amounts. Quite strong correlation was obtained between LTE and number of punchouts as shown in Figure 2.3-(b). In this analysis, all the other variables were kept constant except for longitudinal reinforcement, which varied from 0.5% to 0.6% and 0.7%. A larger amount of reinforcement resulted in decreased crack spacing and smaller crack width, with larger LTE and fewer punchouts. Because a number of variables are involved in CRCP structural behavior and punchout development, and their relationship is quite complicated, it was decided that an expanded sensitivity analysis of the punchout development model would be beneficial in understanding how much sensitivity each variable has on punchout. The results of the sensitivity analyses are discussed next.

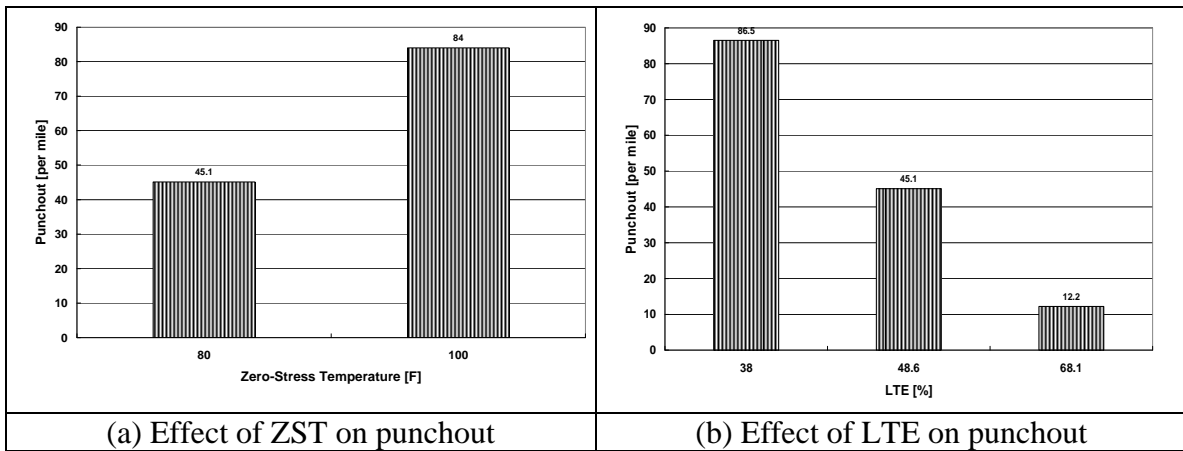


Figure 2.3: Effect of ZST and LTE on punchout

2.3 Sensitivity Analysis

Because there are a number of input variables in MEPDG, it's beyond the scope of this study to conduct a complete sensitivity analysis of all the input variables. Rather, analyses were conducted for the variables that are considered to have substantial effects on LTE and punchouts. These variables include zero-stress temperature (ZST), built-in curling (BIC), slab thickness, and longitudinal steel reinforcement. The input values selected for the sensitivity analyses were those from the test section in the rigid pavement database, 3US287-1, except for the values under investigation.

2.3.1 Effect of Zero-Stress Temperature on CRCP Behavior and Punchout

Figure 2.4-(a) shows the effect of construction month on zero stress temperatures. The ZST values in this figure are computed within MEPDG for months from January through July 1970, for the Wichita Falls environment. The ZST of the concrete placed in January 1970 was estimated at 63 F, while the value was 120 F for concrete placed in July 1970. This information clearly indicates the effect on ZST of the concrete placement season. Figure 2.4-(b) illustrates the effect of ZST on punchouts. The ZST values in the x-axis are those from January (the lowest) to July (the highest) placed concretes. This indicates substantial effects of ZST on punchouts. The effect of ZST on punchout is also substantial, even though subsequent environmental conditions after concrete placements at different months will be different and have some effect on structural responses of CRCP. ZST almost doubled from January placement to July placement and resulting punchout almost quadrupled.

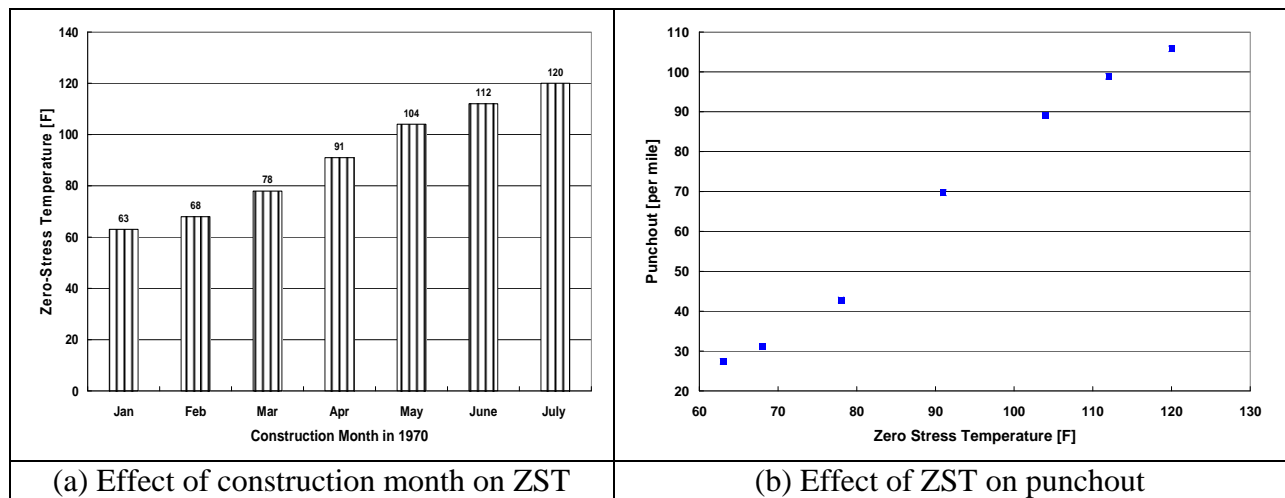


Figure 2.4: ZST effects

ZST refers to the concrete temperature where concrete experiences zero stress after setting. During the concrete setting process, internal concrete temperature increases due to the heat of hydration, which induces the expansion of concrete. By the time concrete obtains the highest temperature during the hydration process, the concrete is usually in compression due to the concrete expansion and the restraint provided by the mass of concrete. Once temperature starts to drop, the compressive stresses decrease, and at some point, there will be zero stress in concrete before tensile stresses develop. This temperature where concrete experience does not experience stress, or the temperature at which concrete stress changes from compression and

tension, is defined as ZST. It is postulated that this temperature is quite important in CRCP behavior and performance, because crack spacing and crack width, and the resulting LTE and other performance parameters, will depend on this temperature. In MEPDG, ZST is estimated from cementitious material content and mean monthly temperature for month of construction as shown in Equation (2.1).

$$T_z = 0.202*CC*H+MMT \tag{2.1}$$

where T_z = zero stress temperature, F
 CC = cementitious material content, lbs/cy
 $H = -0.0787+.007*MMT-0.00003*MMT^2$
 MMT = mean monthly temperature for month of construction, F

Equation (2.1) shows that the mean monthly temperature for month of construction has a direct effect on ZST. The term H increases until MMT reaches 117 F. Because mean monthly temperature in Texas does not exceed 117 F, equation (2.1) implies ZST is almost proportional to mean monthly temperature. It appears that the way ZST is estimated in MEPDG is overly simplified. Actual ZST was measured under TxDOT 0-1700 research study. Figures 2.5-(a) and 2.5-(b) show actually measured ZST in Austin and Cleveland sections, respectively. In these experiments, concrete total strains were measured, along with stress-independent strains (temperature and moisture-induced strains). The stress-independent strains were subtracted from the total strains to obtain stress-dependent strains. The results show that ZST is quite close to the maximum concrete temperature during hydration. This finding corroborates the findings from Springenschmid and Breitenbucher (1995) (3). They suggested that average zero-stress temperature is about 95.5% of the concrete maximum temperature.

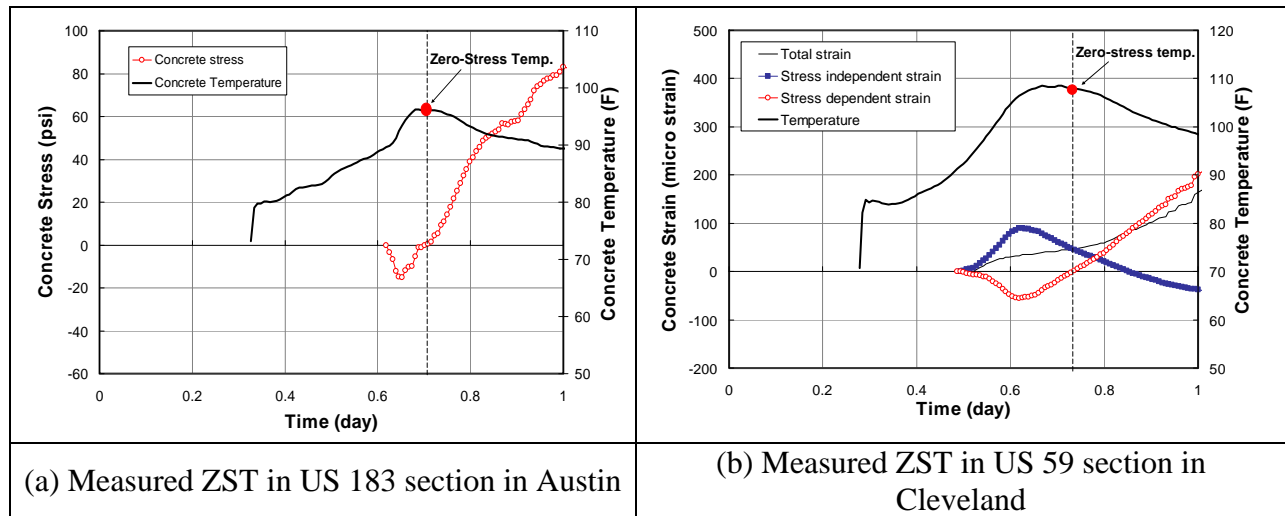


Figure 2.5: Measured ZST

The preceding discussion indicates that, for all practical purposes, the maximum concrete temperature due to heat of hydration after concrete placement can be assumed as ZST. Field measurements of concrete setting temperature and ZST obtained in TxDOT research project 0-1700 indicate a large variability within a single day. Figure 2.6 shows concrete temperature

variations at 1 in. from the slab surface over time for concrete placed on July 20, 2003, on US 59 in Cleveland of the Houston District. It shows a difference of 16 F in maximum concrete temperatures placed at 10:00 a.m. and 2:00 p.m. According to Figure 2.4-(b), this difference of maximum concrete temperature or ZST could result in the difference of 24 punchouts per mile for the pavement structure in Wichita Falls. This presents a question of whether the ZST estimation method in equation (2.1) using mean monthly temperature is a right approach. At the same time, because ZST varies to a large extent in concretes placed within a day as shown in Figure 2.6, and because ZST has such a substantial effect on punchout as shown in Figure 2.4-(b), this area of ZST and its effect on CRCP behavior and punchout needs to be further investigated. Up to this point, almost no research effort has been conducted in this area of ZST and CRCP performance. Currently, efforts are underway in TxDOT research study 0-5832 to further study ZST and its relation to CRCP behavior and performance. In that study, ZST will be measured in actual pavements, and CRCP behavior in terms of cracking, crack width development, and variations in LTE will be measured. It is expected that the study will provide valuable information in this important area.

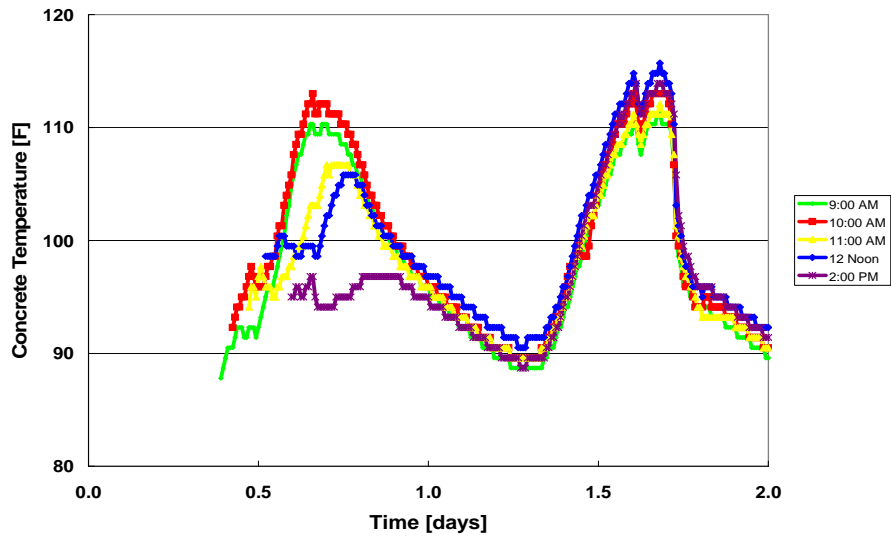


Figure 2.6: Variations in temperature of concrete placed at different times of day

The reason why ZST has such a substantial effect on punchouts in MEPDG is that it has a direct impact on crack width. In MEPDG, crack width is derived from the equation (2.2). In this equation, the *drop in temperature* term is computed by subtracting concrete temperature at any time from ZST of that portion of concrete. It follows that the higher the ZST, the larger the value in the drop in temperature term, resulting in larger crack width. Larger crack width will result in reduced LTE and more punchouts.

$$cw_i = CC \cdot \bar{L} \left(\varepsilon_{shri} + \alpha_{PCC} \Delta T_{\zeta m} - \frac{c_{2i} f_{\sigma}}{E_{PCCi}} \right) \cdot 1000 \quad (2.2)$$

If $cw_i < 0$, $cw_i = 0$

where

- cw_i = average crack width at the depth of the steel for monthly increment i , mils
- CC = local calibration constant (CC=1 is used based on global calibration)
- \bar{L} = mean crack spacing, inch
- ε_{shri} = unrestrained concrete drying shrinkage at the depth of the steel for monthly increment i , "strains"
- α_{PCC} = PCC coefficient of thermal expansion, °F⁻¹
- $\Delta T_{\zeta m}$ = drop in PCC temperature from the concrete "set" temperature at the depth of the steel for each month m , °F
- c_{2i} = second bond stress coefficient for monthly increment i
- $f_{\sigma i}$ = maximum longitudinal tensile stress in PCC at the steel level for monthly increment i
- E_{PCCi} = PCC elastic modulus for monthly increment I , psi

This equation first estimates concrete compressive strains due to temperature drop and moisture loss and concrete tensile strains by concrete stresses. It then subtracts concrete tensile strains from compressive strains. The results are multiplied by the length of the concrete slab between two adjacent transverse cracks, which becomes crack width. However, there are several issues that need to be discussed in this equation.

First, the equation (2.2) assumes that all the concrete between two transverse cracks contributes to crack widths. However, field testing conducted under TxDOT research study 0-1700 illustrates that restraints on concrete volume changes by longitudinal steel are limited to about 12 inches from transverse cracks, although this distance might vary depending on the environmental loading. Steel strains were evaluated in longitudinal steel as shown in Figure 2.7-(a) (Nam 2005). Steel strain gages were installed at 0-in., 6-in., 12-in., 18-in., and 24-in. from the induced transverse crack. Figure 2.7-(b) illustrates the steel strains at different distances from a transverse crack. It shows that steel strains remain almost zero beyond 12 inches from the transverse crack. This indicates that concrete volume changes contributing to crack widths at the steel depth is limited to about 12 inches from a transverse crack.

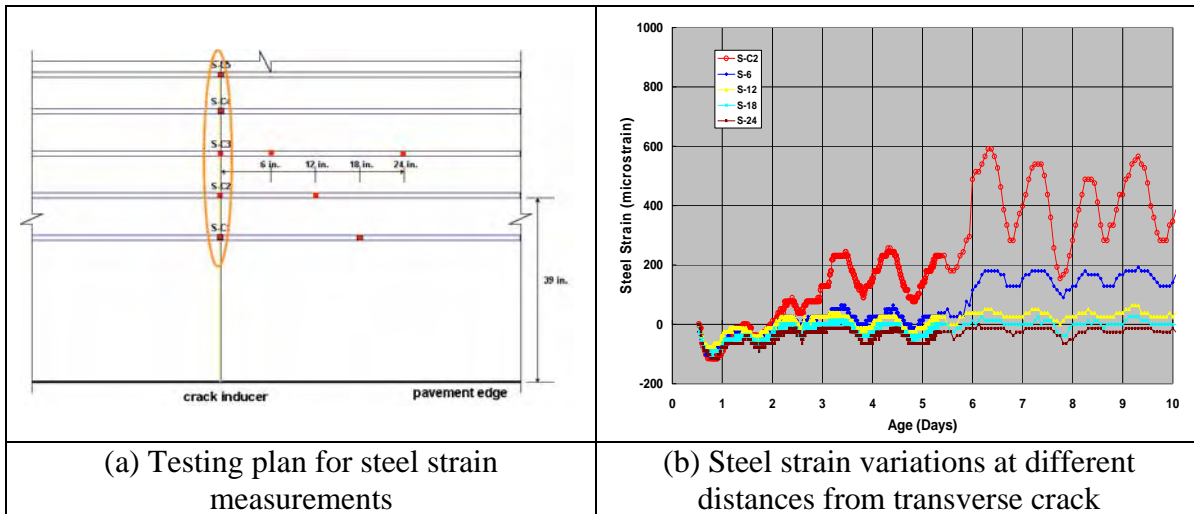


Figure 2.7: Steel strain measurements and variations

This finding explains what has been observed in TxDOT research study 0-1244 (4). In that study, DEMEC gages were installed continuously for over 10 ft in a longitudinal direction. When two cracks developed within this area, the movements of concrete were measured between DEMEC gages.

Figure 2.8-(a) shows that the slab movement is confined near the transverse crack area, which confirms the findings shown in Figure 2.7-(b). In other words, as long as crack spacing is larger than 2 ft, the effect of crack spacing on crack width will be negligible. This could explain a poor correlation between crack spacing and crack width as shown in Figure 2.8-(b). Recall that the equation (2.2) implies approximate linear relation between crack spacing and crack width, while Figure 2.8-(b) shows otherwise.

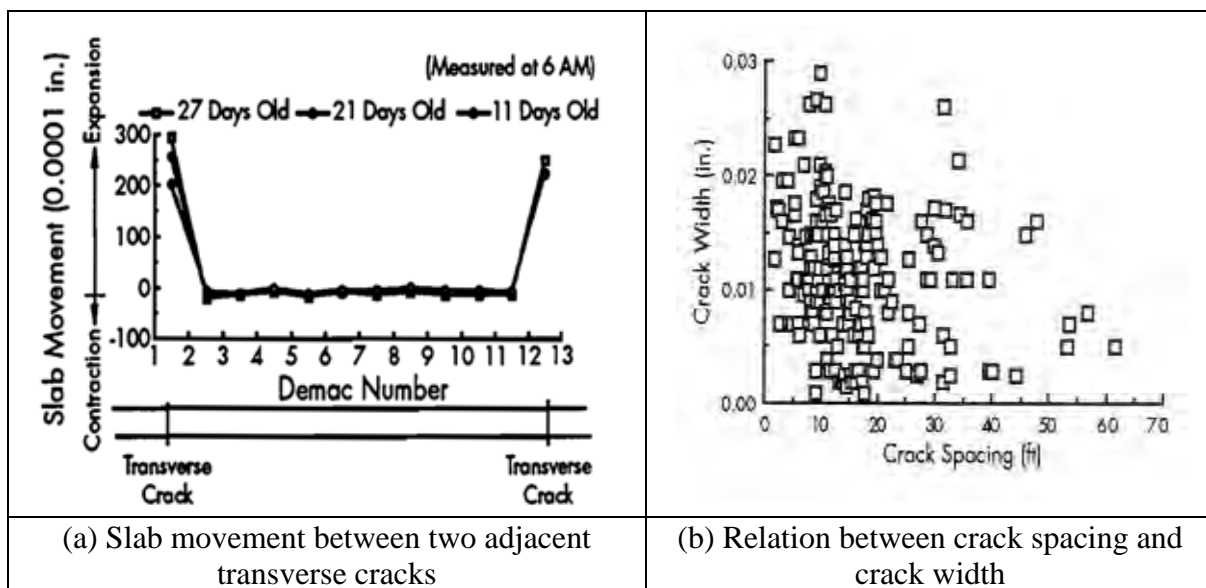


Figure 2.8: Crack data

The second discussion item on equation (2.2) is the way the drying shrinkage effect is incorporated. In equation (2.2), the accumulated drying shrinkage value from the concrete setting is used. In other words, equation (2.2) assumes that all the cracks occur right after setting, and no more cracks will develop in CRCP, which is not the case. Depending on the environmental condition and the effectiveness of curing operations, some cracks could form quite late. To illustrate the effect of the timing of crack development on crack width, assume that cracks form at early ages. Then, subsequent drying shrinkage will make the crack widths larger compared with cracks that form much later, when drying shrinkage is almost complete. Figure 2.9-(a) shows the actual drying shrinkage measured in the field (5). For a crack that occurred at 2 days after concrete placement, there will be additional 200 micro-strains of drying shrinkage at 30 days. On the other hand, if a crack occurred at 14 days after concrete placement, additional drying shrinkage at 30 days will be about 70 micro-strains, and the drying shrinkage up to the 14th day (in this case, about 180 micro-strains) was absorbed by the creep of concrete. The resulting width of the crack that occurred at 14 days will be smaller compared with the width of crack that occurred at 2 days, if the crack spacing is comparable. As discussed earlier, equation (2.2) implies an approximate linear relationship between crack spacing and crack width; however, field-measured values show otherwise, as shown in Figure 2.9-(b). This discrepancy could be a result of not including the time of crack-forming effect of drying shrinkage in the equation (2.2). Because equation (2.2) uses drying shrinkage value from the setting of the concrete, it over-predicts actual crack widths as explained above.

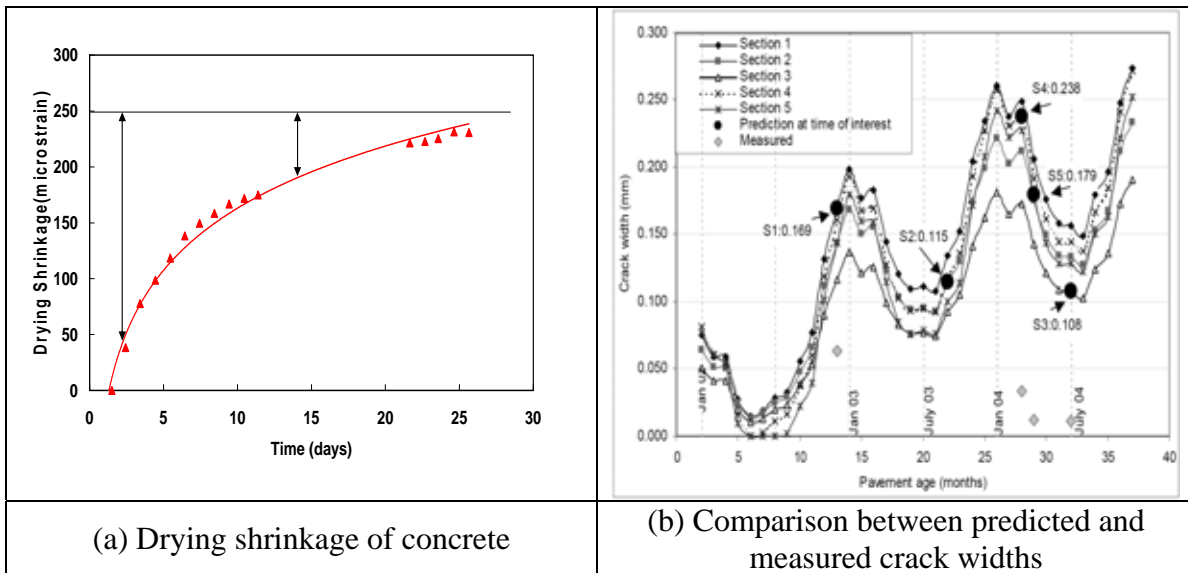


Figure 2.9: Shrinkage and crack widths

A research study at by Kohler et al. at the University of Illinois (6) compared crack widths predicted by MEPDG with actual measurements. Figure 2.9-(b) illustrates the comparison. It shows a large discrepancy between actual measurements and predicted values, as much as more than 10 times. The over-prediction of crack width by MEPDG could be due to the combined effects of two factors explained earlier.

The third discussion item is that the equation (2.2) assumes that crack widths increase over time, primarily due to the continued drying shrinkage of concrete. However, field evaluations of crack width over time indicate that crack widths actually decrease over time. The

detailed information is included in the report 0-5445-2. The exact reason for this reduction in crack width over time is not completely known, even though it is postulated that tensile creep could play a role.

The equation (2.2) could be improved by (1) making drying shrinkage as a function of time, so that crack width will depend on when the crack forms and (2) limiting the concrete area that contributes to crack width. Once a more reasonable equation is developed for crack width prediction, the effect of ZST on crack width, LTE, and punchout could be reduced, potentially substantially.

2.3.2 Effect of Built-in Curling on CRCP Behavior and Punchout

When plastic concrete sets, the concrete temperature distribution through the slab depth is not uniform. There will be temperature gradient at setting and subsequent stress development will be based on the temperature variations from the temperature gradient at setting. This temperature gradient is defined as built-in curling (BIC). BIC is different from ZST distribution through the slab depth, because there are differences between setting temperatures and ZST. The introduction of zero-stress temperatures and built-in curling to CRCP research is rather recent, and no published data from actual CRCP is available. As discussed earlier, efforts are currently under way in TxDOT research study 0-5832 to measure zero stress temperatures and built-in curling in CRCP projects. In MEPDG, BIC is set at -10 F, which is the value derived from curling measurements in LTPP database. As in ZST, Figure 2.10 illustrates the effect of BIC on punchouts, which shows that BIC's effect on punchout is not small.

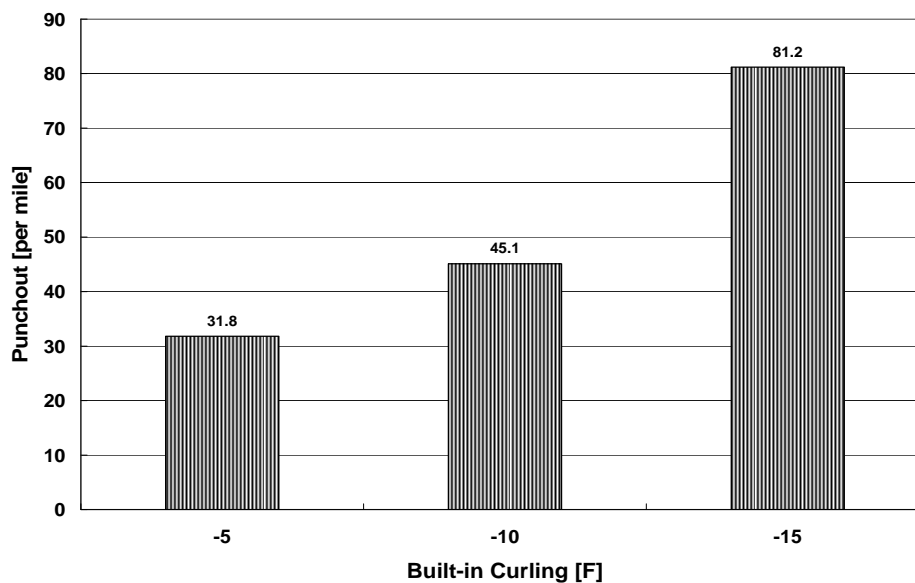


Figure 2.10: Effect of built-in curling on punchouts

2.3.3 Effect of Slab Thickness and Steel Percentage on CRCP Behavior and Punchout

Figures 2.11-(a) and 2.11-(b) show the effects of slab thickness and longitudinal steel amount on punchouts. Increasing the slab thickness from 8-in. to 9-in. reduces punchout from 45.1 per mile to 3.5 per mile. If the thickness is increased to 10-in., there are almost no

punchouts. The effect of slab thickness is quite substantial, potentially even more than observed in the field. The effect of longitudinal steel is not as significant as slab thickness is. Increasing longitudinal steel amount from 0.6% to 0.7% reduces punchout from 91.9 to 45.1 per mile.

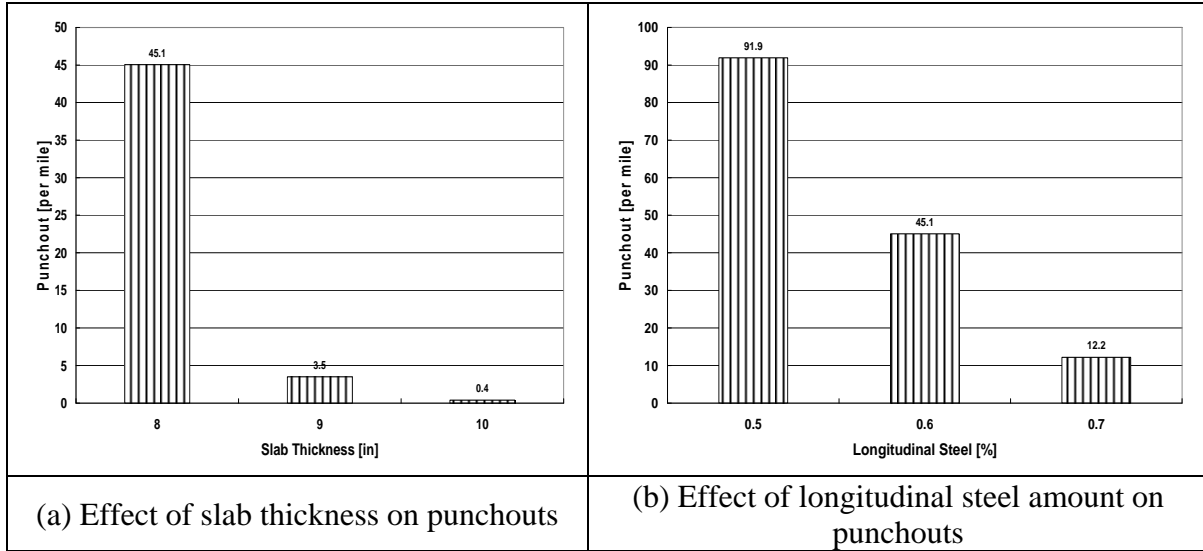


Figure 2.11: Effects on punchouts

The marked effect of slab thickness on punchout in MEPDG is explained by the direct and substantial effect of slab thickness on LTE. On the other hand, the longitudinal steel amount does not have as much effect as thickness has on LTE. This difference is due to the fact that the contribution of longitudinal steel to LTE and crack stiffness is not direct, as slab thickness is. Longitudinal steel has indirect effect on LTE through its effect on crack width control. LTE estimation in MEPDG is through transverse crack stiffness, which is estimated by equation (2.3):

$$\text{Log}(J_{ci}) = ae^{-e\left(\frac{J_s-b}{c}\right)} + de^{-e\left(\frac{s_i-e}{f}\right)} + ge^{-e\left(\frac{J_s-b}{c}\right)} \cdot e^{-e\left(\frac{s_i-e}{f}\right)} \quad (2.3)$$

Where:

- J_{ci} = transverse crack stiffness for monthly increment i , $(AGG/k)_c$
- s_i = adjusted shear capacity computed for the current monthly increment i .
- J_s = stiffness of the shoulder/lane joint from Table E, $(AGG/kl)_s$.

Table E. Stiffness of the shoulder/lane joint.

Shoulder type	$(AGG/k)_s$
Granular	0.04
Asphalt	0.04
Tied PCC	4

The constants a through g are regression constants and the values are as follows:
a = -2.20, b=-11.26, c=7.56, d=-28.85, e=0.35, f=0.38, and g=49.80.

Equation (2.3) shows that, for a given shoulder type and how it is tied to main-lane slab, crack stiffness loss depends on shear capacity loss at the crack only. Shear capacity loss is computed by the equation (2.4). It is shown that, depending on the ratio of crack width to slab thickness, two different equations are used for the shear capacity loss.

$$\Delta s_i = \sum_j \left(\frac{0.005}{1 + 1 \cdot \left(\frac{cw_i}{h_{PCC}} \right)^{-5.7}} \right) \left(\frac{n_{ji}}{10^6} \right) \left(\frac{\tau_{ij}}{\tau_{ref i}} \right) ESR_i \quad \text{if } cw/h_{PCC} < 3.8 \quad (2.4)$$

$$\Delta s_i = \sum_j \left(0.004 + \frac{0.068}{1 + 6 \cdot \left(\frac{cw_i}{h_{PCC}} - 3 \right)^{-1.98}} \right) \left(\frac{n_{ji}}{10^6} \right) \left(\frac{\tau_{ij}}{\tau_{ref i}} \right) \cdot ESR_i \quad \text{if } cw/h_{PCC} > 3.8$$

where,

- Δs_i = loss in shear capacity during monthly increment i due all load applications j
- cw_i = Crack width calculated for each monthly increment i , mil.
- h_{PCC} = PCC thickness, in
- n_{ji} = Number of efficient axle load applications for monthly increment (i) and load level (j) (no traffic wander).
- τ_{ij} = NN corner shear stress on the transverse crack due to load level (j) during monthly increment (i)
- $\tau_{ref i}$ = Reference shear stress derived from the PCA test results for monthly increment i
- ESR_i = equivalent shear ratio that is an adjustment factor for lateral traffic wander.

$$ESR_i = a + \frac{b}{L} + C \frac{LTE_{ci}}{100}$$

$$a = 0.0026\mu_{wp}^2 - 0.1779\mu_{wp} + 3.2206$$

$$b = 0.1309Ln(\mu_{wp}) - 0.4627$$

$$c = 0.5798Ln(\mu_{wp}) - 2.061$$

where,

- L = 24 inches (2 feet) crack spacing, in
- ℓ_i = Radius of relative stiffness, in
- LTE_{ci} = Transverse crack load transfer efficiency due to aggregate interlock for monthly increment i , %
- μ_{wp} = Mean wheelpath, in

The equation (2.4) indicates that slab thickness is a direct input for shear capacity loss estimation, while longitudinal steel is not a direct input; rather, its effect is included through crack widths. Whether slab thickness has such a substantial effect on punchout, as shown in Figure 2.11-(a) needs to be verified.

2.4 Discussion

In this chapter, the punchout model in MEPDG has been reviewed and sensitivity analyses conducted. During the sensitivity analyses, it was observed that MEPDG results indicate large variations in LTE over time and also within a year (summer vs. winter) as shown in Figure 2.2-(b). It was also observed that there was a good correlation between LTE and crack width variations, as shown in Figures 2.2-(a) and 2.2-(b). On the other hand, in all 27 test sections where detailed LTE was evaluated in this project, LTE values were maintained at high levels—above 95% except for one crack in the winter—regardless of pavement age (from 4 to 38 years), slab thickness (from 8 to 15 inches), crack spacing (small, medium, and large) and the season (summer and winter). This discrepancy is quite significant, and further discussion is warranted. A study by Zollinger and Barenberg (7) states that the load transfer contribution of the reinforcing bar should be ignored. It implies that LTE in CRCP is achieved solely by aggregate interlock, which could be true only when longitudinal steel is completely ruptured. In this database project, no ruptured longitudinal steel was observed, even in 38-year-old 8-in. CRCP on US 287 in the Wichita Falls and Fort Worth Districts. In a US 287 section in the Fort Worth District, a transverse crack was quite wide, but coring showed no steel rupture, even though the aggregate interlock was apparently lost. Figure 2.12-(a) shows the evidence of spalling at the top and bottom of the slab potentially due to excessive deflections. It also shows that the transverse crack went through all the way the slab depth, which is not usually the case in CRCP in Texas. Also shown is the evidence of minor steel corrosion. Figure 2.12-(b) shows that spalling formed on the concrete slab surface as well at the bottom. It also shows asphalt subbase and transverse crack formed along the transverse steel. It illustrates that even though crack width is quite large on the surface, concrete surrounding the longitudinal steel is quite sound, with no evidence of pull-out failure or bearing failure around the steel. LTE was evaluated at this crack. FWD testing conducted at this crack location indicated a void under the slab as indicated by more than 10 mils of deflections. However, LTE was still at 80%. At this crack, because coring shows that transverse crack was wide all the way through the slab depth, and it appears that the aggregate interlock was completely lost, the only component contributing to LTE was longitudinal reinforcement. Recall that there was a void under the slab and, therefore, it is assumed that there was no contribution by subbase to LTE. It can be assumed that, in CRCP with 0.6% longitudinal steel, a minimum LTE of 80% is the lower boundary when the steel is not ruptured with voids under the slab.



Figure 2.12: Core and spalling

LaCoursiere et al. (8) conducted extensive field evaluations of CRCP performance in Illinois and reports large amounts of longitudinal steel failures at transverse crack. The sections evaluated were 5 to 14 years old, with thickness varying from 7 to 10 inches. The applied traffic varied from 2.0 million ESALs to 23.8 million ESALs. However, the study does not provide information on the amount of longitudinal steel used in the sections. When the longitudinal steel ruptures, steel no longer provides load transfer and aggregate interlock is the only mechanism for load transfer. In Texas, longitudinal steel rupture is quite rare or hasn't been observed during this research.

As shown in Figure 2.3, a strong correlation appears to exist between LTE and punchouts. Considering the punchout mechanism in MEPDG, it's not surprising that LTE has such a substantial effect on punchouts, which necessitates the need for accurate evaluation of LTE in the field for the calibration of the punchout model. In the database research study, however, it was discovered that there is a serious discrepancy between LTE values predicted by MEPDG and measured values. LTE values evaluated in the field were maintained at quite high levels in all test sections—above 95% except for one crack in the winter—regardless of pavement age (from 4 to 38 years), slab thickness (from 8 to 15 inches), crack spacing (small, medium, and large) and the season (summer and winter). On the other hand, LTE values predicted by MEPDG as shown in Figure 2.2-(b) are decreasing rather constantly, leading to quite a low value just after 20 years.

Equation (2.5) shows the equation for LTE adopted in MEPDG.

$$LTE_{TOT1} = 100 * \left(1 - \left(1 - \frac{1}{1 + \log^{-1} \left[\frac{0.214 - 0.183 \frac{a}{\ell_1} - \log(J_{ct}) - R}{1.18} \right]} \right) \left(1 - \frac{LTE_{Base}}{100} \right) \right) \quad (2.5)$$

where LTE_{TOTi} = transverse crack load transfer efficiency due to aggregate interlock, reinforcement, and base for monthly increment i , %

li = radius of relative stiffness computed for monthly increment i , inch

Jci = transverse crack stiffness computed for monthly increment i

a = typical radius of a loaded area (6 inches)

R = residual factor to account for residual load transfer provided by the steel reinforcement. $R = 500P_b - 3$

P_b = percent of longitudinal reinforcement expressed as a fraction

LTE_{Base} = load transfer efficiency contributed by the base layer

LTE_{Base} is 20% for aggregate base, 30% for asphalt or cement treated subbase, and 40% for lean concrete subbase. In Equation (2.5), radius of loaded area, radius of relative stiffness, and load transfer efficiency contributed by the base layer remain almost constant throughout the analysis period. Therefore, the only variable responsible for the deterioration of LTE over time in this equation is the changes in transverse crack stiffness. Figure 2.13 illustrates the variations in LTE for a wide range of transverse crack stiffness values. It shows relatively little effect of crack stiffness on LTE when it is larger than 20. On the other hand, once transverse crack stiffness is reduced below 20, LTE decreases rather quickly, and this could explain rather rapid increase in the frequency of punchout in MEPDG results as CRCP reaches its terminal condition. This implies that once transverse crack stiffness has deteriorated, longitudinal steel does not provide adequate LTE. This could be possible only if longitudinal steel is ruptured or the concrete around longitudinal steel at transverse cracks is much deteriorated. In Texas, neither longitudinal steel rupture nor concrete deterioration around longitudinal steel at cracks was observed often. As a matter of fact, it's extremely rare to see either situation. Even when either condition is observed, it's quite localized and often due to locally deficient subbase support condition. It wouldn't be prudent to develop pavement designs to address isolated issues related to construction quality that is not likely to happen often. Otherwise, the pavement design will be more conservative than is needed. As long as longitudinal steel is not ruptured, LTE would be maintained at quite a high level.

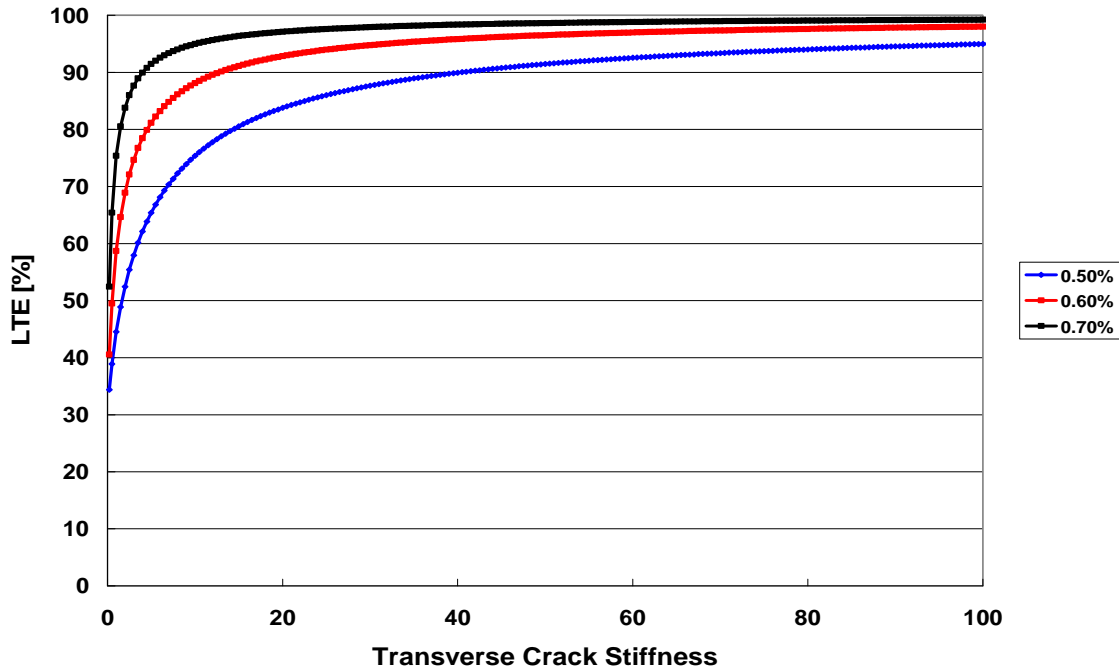


Figure 2.13: Effect of transverse crack stiffness on LTE

Crack width has been cited as one of the most important variables affecting CRCP performance. Unfortunately, not much actual field information is available on the correlation between crack width and punchout. In fact, the information on crack width in actual CRCP is quite limited; almost all the crack widths reported were measured on the surface. The work done under TxDOT 0-1700 and the Kohler work at the University of Illinois discussed earlier are the only efforts to measure crack width at the depth of longitudinal steel. Because the crack width model in MEPDG is for the values at the depth of steel, and the data from TxDOT 0-1700 and the University of Illinois study were not yet available for the national calibration of the MEPDG model, no calibration was ever conducted for the crack width model in MEPDG. As discussed, data from TxDOT research study 0-1700 indicates the closing of cracks over time, which field observations of cracks in old CRCP support. It appears that efforts should be made to measure crack widths at the depth of steel in a number of projects over time, so that the data can be used to calibrate any crack width models. At the same time, it would be desirable to develop a new crack width model, or modify the model included in the MEPDG to address the issues discussed in this chapter. If crack width is more important in protecting steel from corrosion than LTE, then crack width model should be modified accordingly. Any crack width prediction model has to be calibrated with actual data, and without field data, the reasonableness of any crack width prediction models will be in question. Recall that LTE values at all the test sections evaluated in this database project were all above 95%, except for one crack in Test Section 4I40-1, which is in the Amarillo District and had 88% in the winter testing.

Another study conducted at the University of Illinois (6) revealed that LTE was maintained at quite high levels, above 95% as shown in Figure 2.14, and the high LTE was maintained even after punchout failure had occurred. The findings in that study corroborate well with the findings in this database project, which is that LTE values of the cracks in all test sections were maintained at quite high levels. All these findings strongly indicate that high LTE

in CRCP is maintained as long as longitudinal steel is not ruptured. LTE values might go down below 80% only after longitudinal steel is ruptured with voids underneath.

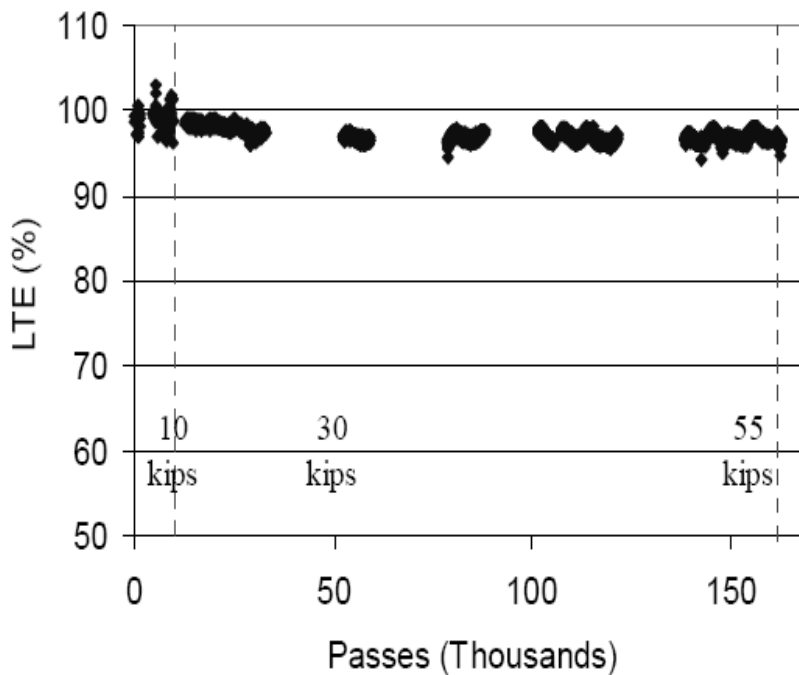


Figure 2.14: Variations of LTE up to punchout development

It appears that the LTE model in MEPDG is based on the study by Portland Cement Association (PCA). The PCA study investigated the LTE of a transverse contraction joint through a large scale experiment. In the study, a transverse joint was induced by placing a 1-in. high galvanized metal strip at the bottom of the slab and providing 1-in. deep grooving on the surface of plastic concrete. Two types of subbase were used: sand-gravel and cement-treated. Two slab thicknesses, 7-in. and 9-in., were used. Joint width was controlled by steel rods anchored in the concrete that were connected through threaded couplings to crossbars at the ends of the box. No dowels were installed at the joint. The findings include a good correlation between joint width and LTE through aggregate interlock. Even though the findings of the PCA study are quite valuable in understanding the mechanisms of LTE at discontinuities in PCC slab, the findings may not be directly applicable to predict LTE in CRCP. As long as an adequate amount of longitudinal steel is used, steel rupture is not likely. At least in Texas, steel rupture has been extremely rare. The only steel rupture observed by the research team in CRCP currently in service was in the area of poor subbase support and resulting slab subsidence. Even the wide transverse crack in the 8-in. CRCP under heavy truck traffic with voids underneath shown in Figure 2.12-(a) has not experienced steel rupture. On the other hand, many steel rupture problems were reported in Illinois. The report by LaCoursiere et al. states that the wide cracks where steel ultimately ruptures are believed to be caused by a combination of factors, including high tensile stress caused by cold temperature and shrinkage, loss of support at the crack, high deflections, corrosion of rebars, heavy repeated traffic loads, and pumping of the subbase. It appears that as long as an adequate amount of longitudinal reinforcing steel is used along with stabilized subbase and tied-concrete shoulders, steel rupture and resulting low LTE might be

avoided. As will be discussed in the next chapter, a punchout mechanism different from the one in the MEPDG has been observed in Texas. In this mechanism, it appears that large slab deflections cause breakage of concrete at the depth of the longitudinal steel, resulting in horizontal cracking at the depth of steel and eventual punchout.

In MEPDG, zero-stress temperature and built-in curling have substantial effects on punchout development, and accordingly affect slab thickness design. Field testing conducted in this project, in terms of deflections and LTE, has not revealed noticeable differences between a 500-ft segment before the construction joint and the 500-ft after the construction joint. In other words, no practical difference was observed in slab deflections and LTE between the two segments, even though ZSTs could have been quite different between the two segments (see Figure 2.6). It is possible that if the subbase support is quite uniform throughout the project, then zero-stress temperature and built-in curling could have primary effects on punchout development. However, based on the observations of punchouts in Texas, which is the subject of the next chapter, subbase support is not uniform throughout the project, and it is postulated that the locations of pumping are affected by roadway geometry in terms of drainage characteristics and local subbase and subgrade condition. It is further postulated that slab deflections have effects on edge pumping. A study in Illinois also confirmed that more pumping and punchouts were observed as slab thickness was decreased. The fact that (1) the punchout locations are not clustered near the transverse construction joints, where zero-stress temperature and built-in curling could be the highest, and (2) slabs with smaller thickness experienced more edge pumping and punchouts, indicates more dominant effects of subbase support and lesser effects of zero-stress temperature and built-in curling on punchouts. It appears that the reason for substantial effects of zero-stress temperature and built-in curling on punchouts in MEPDG is that erosion is independent of slab thickness or traffic. As discussed earlier, in MEPDG, subbase/subgrade material properties and rainfall are the only variables affecting erosion. Once the effect of slab thickness and traffic is included in the prediction of erosion, it appears that the effect of zero-stress temperature and built-in curling could be changed. On the other hand, if the subbase is almost non-erodible and tied concrete shoulder is used as is the case in the new CRCPs in Texas, zero-stress temperature and built-in curling could have effects on punchout, even though the punchout mechanism will be substantially different from the one in MEPDG. Also, the effect of longitudinal steel on the surrounding concrete due to wheel loading applications should be considered, because there is strong field evidence that longitudinal cracking which induces punchout could be due to the effect of continuous longitudinal steel due to wheel loading applications. This will be further discussed in the next chapter.

Based on the findings in this chapter, it appears that it's premature to try to calibrate the punchout model using the data from this project. Rather, in-depth discussion on punchout mechanism is in order, which will be the subject of the next chapter.

Chapter 3. Calibration of Punchout Model

In this chapter, efforts made to calibrate the MEPDG punchout model using information collected in this project are described. In this database project, punchouts were not frequently observed, especially in the sections built since 1980s where improved design features such as tied-concrete shoulders and stabilized subbase were used; on the other hand, punchouts were observed in a section on US 287 in Wichita Falls District, which was built in 1970. Detailed information was collected for this section, and efforts were made to compare the performance of this section in terms of punchout with that from MEPDG.

3.1 Information Collected for the Calibration of Punchout Model

Calibration of such a complicated model as the punchout model in MEPDG requires detailed information from a number of CRCP sections that experience punchout distresses. As discussed in the previous chapter, the input variables required for MEPDG are far more extensive than those for current TxDOT pavement design procedures. Accordingly, much of the input information needed for CRCP design using MEPDG has not been collected in TxDOT on a routine basis. Also, structural responses that are needed for the calibration of punchout model in MEPDG have not been collected in TxDOT on a routine basis either. Based on the review of the MEPDG punchout model available at the time this database project was initiated, it was decided that the following information on CRCP responses needs to be collected in this project for the calibration of the punchout model:

1. Variations of LTE over time
2. Correlation between LTE and transverse crack spacing
3. Pavement deflections

Because MEPDG shows that LTE has a strong influence on punchout, and that LTE varies depending on the time of year (temperature effects), it was decided that testing would be conducted for LTE in the summer and winter. The detailed testing procedures and results are included in the Report 0-5445-2. As discussed in the previous chapter, MEPDG assumes an almost linear relationship between crack spacing and crack width, which determines LTE. In this project, in each test section, LTE values were measured for three different crack spacings: small, medium, and large. The testing results indicate that, in all test sections, LTE values were maintained over 95% except for one crack in one test section, regardless of slab thickness, pavement age, and crack spacing. The results of the field testing conducted to evaluate LTE are contained in the Appendix A of the report 0-5445-2.

NCHRP 1-37(A) (I) emphasizes the importance of erosion on the punchout, and erosion is an important factor in the punchout model, as erosion was present in many punchouts observed in CRCP in many U.S. states, including Texas. In the past, before stabilized subbase along with tied-concrete shoulder was used in CRCP in TxDOT, edge punchouts were common problems in some CRCP sections due to subbase erosion. And erosion under the concrete slab was a primary cause for pavement distress at the AASHO Road Test. Based on the performance of concrete pavement in the past, it is essential to include the erosion effect in pavement structural analysis. Intuitively, pavement edge deflections must have an effect on erosion—the larger the deflections, the higher the erosion potential for given pavement structure, materials, and environmental

condition. However, the erosion model included in the punchout model does not consider the pavement deflections as a variable as shown in equation (3.1).

$$RE_i = (-0.37 + 0.0171P_{200} + 0.0779EROD + 0.0117PRECIP)/12$$

(if $E < 0$, set $e = 0$)

(3.1)

- RE_i = monthly rate of base erosion from the slab edge, in/month
 P_{200} = percent subgrade passing the no. 200 sieve
 $PRECIP$ = mean annual precipitation, inch
 $EROD$ = erodibility index from the following table.

<i>EROD</i>	Material Description*
1	Lean concrete with 8 percent cement; asphalt concrete with 6 percent asphalt cement, or a permeable drainage layer.
2	Cement treated granular material with 5 percent cement manufactured in plant; asphalt treated granular material with 4 percent asphalt cement.
3	Cement-treated granular material with 3.5 percent cement manufactured in plant; asphalt treated granular material with 3 percent asphalt cement.
4	Granular material treated in place with 2.5 percent cement, treated soils.
5	Untreated granular material.

* Modified from original PIARC recommendations.

In this equation, base erosion is a function of minus 200 material in the subgrade, precipitation, and erodibility index from the table in equation (3.1), which purely depends on base/subbase material characteristics. In short, base erosion is independent of slab deflections. However, the research team felt that slab deflection is an important CRCP structural response that determines not only erosion but other distress-causing structural responses as well. This is because pumping at the pavement edge partly depends on the deflections, among other factors such as erodibility of the subbase material, drainage characteristics, rainfall amount, and shoulder type. Slab deflections were evaluated at every 50 ft along the 1,000-ft long test section.

3.2 US 287 Section in Wichita Falls District

Part of the US 287 section in Wichita Falls District was placed and opened to traffic in 1970. A 1,000-ft long test section was selected from this part of US 287 and a detailed structural evaluation was conducted. Table 3.1 provides general information of the test section.

Table 3.1: General description of Wichita Falls Test Section

GENERAL DESCRIPTION	
Highway	US 287
District	Wichita Falls
County	Wichita
Direction	N
Reference Marker	MP 330
Pavement Type	CRCP
Slab Thickness	8 in
Construction Date	1970-09-01
Vertical Alignment	Grade
Horizontal Alignment	Curve R
No of Lanes	2
PMIC Surveyed Lane	L1
Shoulder Type	Asphalt Concrete
Surface Texture	Transverse tining
Concrete CAT	Sandstone
Drainage	Open ditch
GPS (start)	N33°57'59.7"
	W098°43' 25.8"
GPS (end)	N33°58'03.3"
	W098°43' 36.8"
Survey Dates	2007-01-29
Surveyors	Medina, Suliman, Finley

This section is on northbound US 287, north of Iowa Park. It is 8-in. CRCP over asphalt-treated subbase, with an asphalt shoulder. Figure 3.1 shows the typical condition of the section. Detailed structural evaluation was conducted, which included crack spacing measurements, falling weight deflectometer testing, and load transfer efficiency evaluations. Figure 3.1-(b) illustrates crack spacing distribution. The average crack spacing is 4.7 ft with a standard deviation of 2.4 ft. It shows that transverse crack distribution follows a bell-shaped curve, with 3.3% of the cracks having less than 1-ft spacing and 2.4% of the cracks having more than 10-ft spacing. This wide scatter in transverse crack spacing typifies the characteristics of transverse cracks in CRCP, which underscores the complexity of the transverse cracking mechanisms and the interactions of the variables involved in cracking in CRCP. As discussed in the previous chapter, the punchout mechanism in MEPDG assumes an approximate linear relationship between crack spacing and crack width.

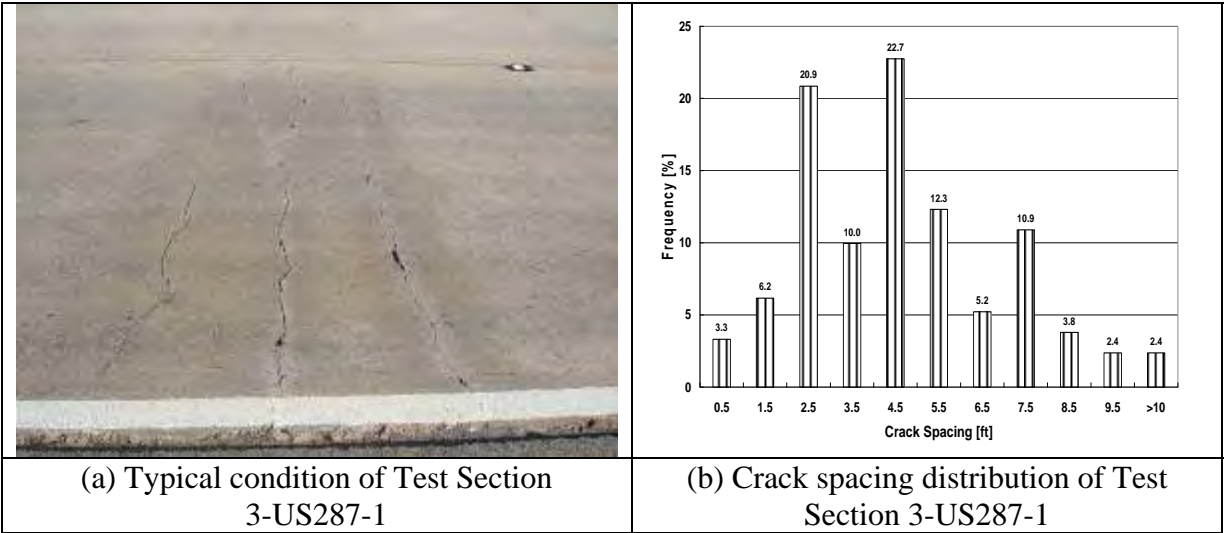


Figure 3.1: Condition of US 287

For cracks with the spacing distribution shown in Figure 3.1-(b), crack widths would follow similar distribution. On the other hand, MEPDG uses an average crack width that corresponds to the average crack spacing for subsequent computations, such as deterioration of load transfer efficiency and crack stiffness, and punchout predictions. It is understandable that structural evaluation of cracks with various spacing would require extensive computation time; however, using a single crack width at a given time for the whole project in punchout prediction could result in erroneous values.

LTE was evaluated in summer 2007 and winter 2008 for three crack spacings: small, medium, and large. Table 3.2 summarizes the results. It shows that LTE values are maintained at quite high levels, almost 100% regardless whether they were evaluated in the summer or in the winter, which contradicts the predictions made by MEPDG shown in Figure 2.2. It also shows that LTE is not dependent on crack spacing. If crack widths depend on crack spacing and have substantial effects on LTE as MEPDG predicts, different LTE values would result for cracks with different spacing. Similar deflections are observed in summer and winter that were measured at cracks for the evaluations of LTE. Deflections measured at 50-ft intervals for the test section show the average deflection of 4.35 mils in the summer of 2007 and 4.19 mils in the winter of 2008. Recall that LTE values predicted by MEPDG are high in the summer and low in the winter. The reason for the seasonal variation in LTE predicted by MEPDG is that LTE depends on crack width, which varies in accordance with temperatures, as shown in the equation (2.2).

**Table 3.2: LTE evaluation at cracks with various spacing
3US287-1**

Crack .	GPS Coordinates		Crack Spacing	
	I.D.	Latitude	Longitude	Before
S-I-1	N 33°58'59.8"	W 098°43'26.5"	2'6"	2'7"
S-I-2	N 33°58'00.0"	W 098°43'27.4"	2'6"	2'6"
L-I-1	N 33°58'00.2"	W 098°43'28.1"	6'3"	6'3"
L-I-2	N 33°58'00.4"	W 098°43'29.0"	8'1"	8'6"
M-I-1	N 33°58'00.8"	W 098°43'29.9"	5'2"	4'11"
M-I-2	N 33°58'01.0"	W 098°43'30.4"	4'0"	4'3"
S-II-1	N 33°58'01.6"	W 098°43'32.1"	2'5"	2'2"
M-II-1	N 33°58'01.4"	W 098°43'32.3"	4'5"	3'2"
L-II-1	N 33°58'01.4"	W 098°43'32.6"	7'5"	7'4"
S-II-2	N 33°58'01.6"	W 098°43'32.8"	1'10"	1'9"
L-II-2	N 33°58'02.2"	W 098°43'34.2"	9'11"	7'3"
M-II-2	N 33°58'02.7"	W 098°43'35.4"	3'11"	3'7"

Crack .	Deflections (Winter)		Deflections (Summer)		%LTE	
	I.D.	du	dl	dl	du	Winter
S-I-1	3.75	3.53	3.70	3.69	106.3	100.3
S-I-2	4.47	4.15	4.07	4.04	107.8	100.7
L-I-1	4.75	4.29	4.03	3.99	111.0	101.0
L-I-2	4.25	3.99	3.89	3.87	106.6	100.5
M-I-1	3.96	3.63	5.38	5.27	109.0	102.1
M-I-2	3.83	3.55	3.82	3.81	107.8	100.3
S-II-1	3.86	3.83	4.06	4.02	100.7	101.0
M-II-1	4.52	4.01	4.28	4.24	112.6	101.0
L-II-1	4.13	3.87	4.29	4.26	106.7	100.7
S-II-2	3.89	3.91	4.22	4.24	99.7	99.4
L-II-2	4.07	3.59	3.94	3.89	113.5	101.4
M-II-2	4.24	3.64	3.96	3.93	116.4	100.7

This section was selected for the evaluation of the MEPDG punchout model for the following reasons:

- 1) This section has an asphalt shoulder, and as described in Chapter 2, the punchout model in the MEPDG is more appropriate for CRCP with asphalt shoulder.
- 2) The section is more than 38 years old and truck traffic has been quite substantial.
- 3) Evidence of pumping was observed with resulting longitudinal cracks and punchouts.

3.3 MEPDG Evaluation of this Section

Structural performance evaluation of this test section was conducted using MEPDG. MEPDG requires rather extensive input information, some of which is not available because this section was built in 1970. However, efforts were made to estimate best values for required input variables. Brief description of the required input parameters in MEPDG and the values selected for this analysis are presented. In MEPDG, there are four categories of the input needed: (1) general information including site identification and analysis parameters, (2) traffic information,

(3) climate, and (4) pavement structures. The information needed for the first category is not used in the actual pavement analysis, except for the construction and “open to traffic” months. The best information available for the construction of this section is September, 1970. This date could quite possibly be the month the project was accepted by TxDOT, and the actual construction could have been a few months prior to the acceptance. Because the construction month has substantial effect on ZST and punchout, as shown in the sensitivity analysis described in Chapter 2, it was necessary to determine the most probable construction month. With the information on construction month not available, attempts were made to estimate the construction month by comparing actual crack spacing with the predictions from MEPDG. Figure 3.2-(a) shows the average crack spacing predicted by MEPDG for different months of construction. The actual average crack spacing is 56.4 inches, and it is assumed that this section was constructed in March 1970. Figure 3.2-(b) shows zero stress temperatures of the section predicted from MEPDG if it had been constructed in different months. The ZST for March 1970 construction in Wichita Falls was estimated at 78 F.

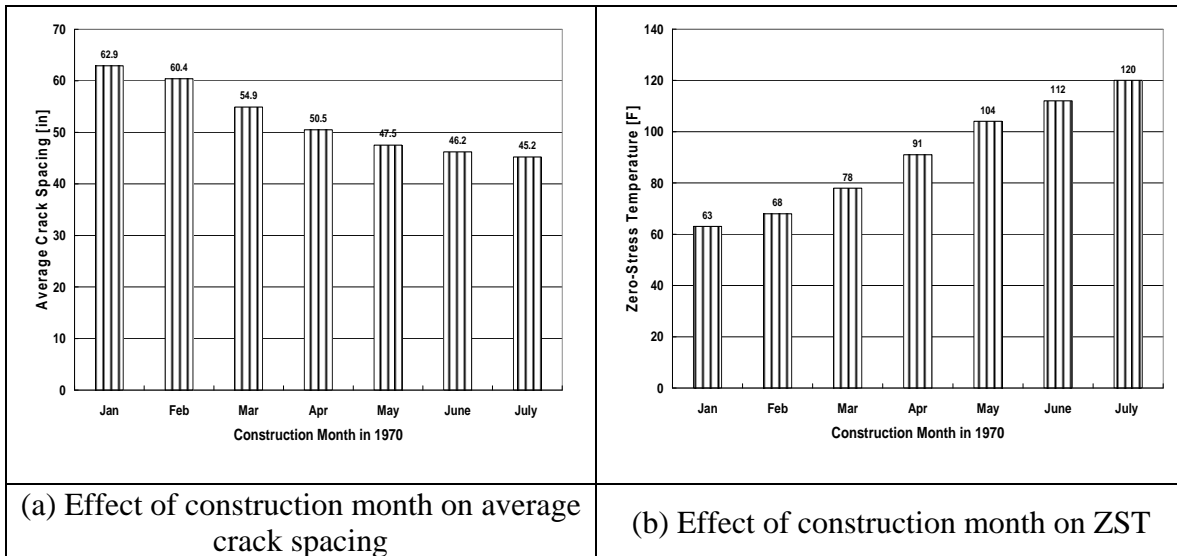


Figure 3.2: Effect of construction month

The current traffic information was obtained from the district pavement engineer. Current average annual daily traffic (AADT) is 16,350, with 34% trucks. To estimate the traffic for this section, it was assumed that there has been 5% annual growth of traffic in this section. The traffic growth analysis shows that there was 2,690 AADT per day in 1970. With the additional assumption of the same percentage of trucks, the initial truck traffic was 914 trucks per day in both directions in 1970. MEPDG requires more detailed information on traffic than the current AASHTO or TxDOT pavement design procedure requires. Such information includes hourly distribution of the trucks for each truck type and traffic wander. The information was not available, and the default values in the MEPDG were selected. As for the climate information, GPS information of this section was provided to the MEPDG and six weather stations were selected for interpolations. The information needed in MEPDG for pavement structure is quite extensive, and not all the information was available. More specifically, information required for concrete materials is more extensive than that normally TxDOT evaluates. They include zero-stress temperatures of concrete, built-in curling, reversible drying shrinkage, and thermal

diffusivity. The values for these input parameters are almost impossible to obtain, because testing might have not been conducted for these parameters during construction in 1970, and even if the testing was done at that time, the information is not available now. If some of these variables have substantial effects on punchout, calibrating the punchout model would be quite difficult or almost impossible. Sensitivity analyses described in Chapter 2 indicates a quite substantial effect of ZST. Even though ZST of 78 F was estimated by assuming that the pavement section was built in March 1970 by comparing actual and predicted average crack spacing, it is not known how accurate this estimate is.

Actual punchout was evaluated in the section that included the 1000-ft test section. The section starts 0.2 miles south of reference marker (RM) 330 and extends 1.6 miles to the north. A total of 2 punchouts was observed in this section, resulting in 1.3 punchouts per mile. This value is substantially smaller than the values obtained in the analyses (42.8 punchouts per mile).

3.4 Discussion

As discussed in Chapter 2, the punchout model in MEPDG is quite complicated and there are a number of calibration constants that need to be adjusted to local conditions. In MEPDG, there are three equations that contain calibration constants: (1) concrete fatigue equation, (2) damage-punchout transfer function, and (3) crack width equation. Among these three equations, concrete fatigue equation has been well established. As discussed in Chapter 2, crack width equation in MEPDG appears to over-predict and the national calibration constant suggested in MEPDG, which is 1.0, needs to be further evaluated. Damage-punchout transfer function has three calibration constants, and determining them will require quite substantial number of sections with punchouts. In this project, an insubstantial amount of punchout information has been collected, and as will be discussed in the next chapter, most of the so-called punchouts observed in the field in Texas are not due to structural deficiency; rather, they are due to imperfections in design details and/or construction/materials quality issues.

In MEPDG, the transfer function for the punchout from accumulated damage is in the form of the equation (3.2).

$$PO_i = \sum_{i=1}^{Life} \frac{a}{1 + b \cdot D_i^c} \quad (3.2)$$

where,

- PO_i = total predicted number of punchouts per mile at the end of i^{th} monthly increment
- D_i = accumulated fatigue damage (due to slab bending in the transverse direction) at the end of i^{th} monthly increment
- a, b, c = calibration constants for the nationally calibrated model (105.26, 4.0, -0.38)

The regression constants a, b, c were derived from the nationwide punchout information in LTPP database. Sensitivity analysis was conducted on those constants with a fixed accumulated fatigue damage of 5.0. In the analyses, values corresponding to the ratios from 0.3 to 2.0 of constants from nationally calibrated model were used. Figure 3.3 shows the results. Within 20% of the nationally calibrated constant values, punchouts vary almost linearly, with about 2 punchouts per mile for 10% deviation of each constant. It was decided that the calibration constants in Texas should not vary from nationally calibrated constants by more than 20%. With that assumption, the maximum difference between actual and predicted punchout

values would be a maximum 8 per mile. However, in this section, the difference is more than 40 punchouts per mile. At this point, it was postulated that there might be other causes for this large discrepancy and efforts were made to identify the potential cause(s) for this large discrepancy. MEPDG allows the user to specify local calibration constant for crack width as shown in equation (2.2). The punchout behavior of this section was analyzed by specifying values from 0.1 to 1.0 with increment of 0.1.

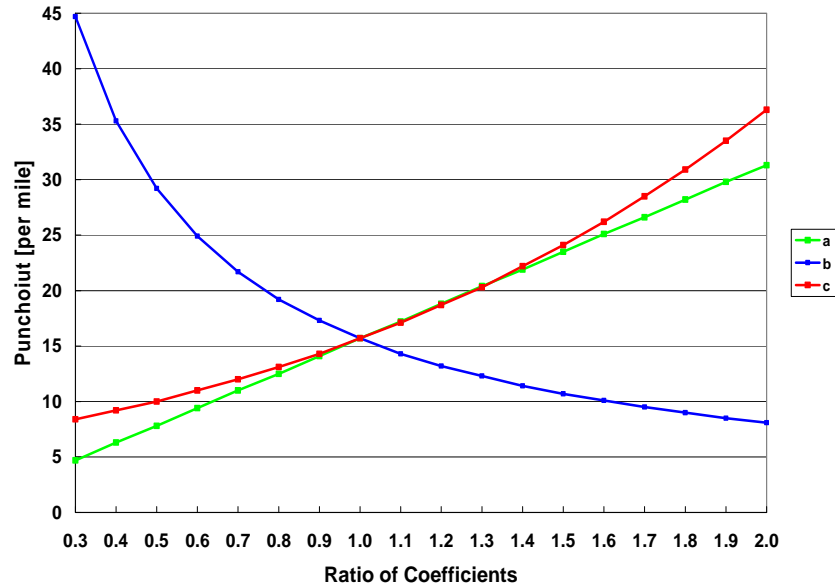


Figure 3.3: Sensitivity of calibration constants on punchout

Figure 3.4-(a) shows predicted crack width and LTE in 2008 as affected by the changes in calibration constant for crack width. MEPDG algorithm appears to work properly, because the crack width increases linearly with the calibration constant. It shows that, in this case, LTE is maintained at quite high levels with a crack width calibration constant up to 0.5. Once the crack width calibration constant gets larger than 0.5, LTE decreases rather quickly.

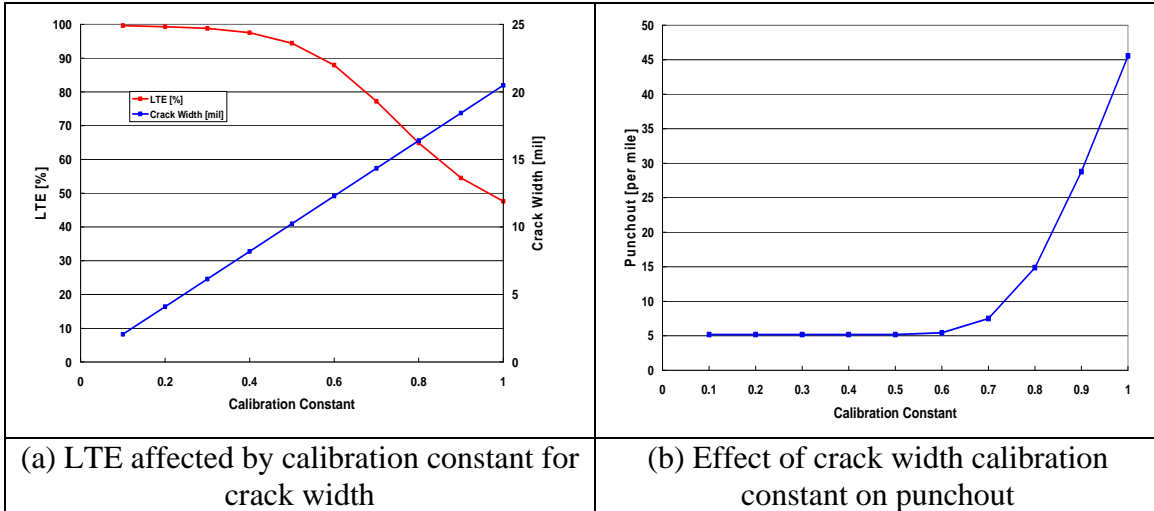


Figure 3.4: Effect of calibration constants

Figure 3.4-(b) illustrates the effect of calibration constant on punchouts. Based on the field measurements of LTE and punchouts, it appears that the calibration constant for crack width could be 0.4 or less, at least for the Wichita Falls section. Recall that, according to University of Illinois study, the crack width values predicted by MEPDG were larger than actual values. This discussion is based on the assumption that the national calibration constants for damage-punchout transfer function can be applied to Texas condition without modifications. Because it appears that punchout information used for the calibration of MEPDG punchout model may not be accurate, which will be discussed in more detail in the next chapter, it's difficult to decide whether the national calibration constants for damage-punchout transfer function can be accepted and used for the calibration of constant for crack width model.

Because the number of sections with enough number of punchouts obtained in this project is quite limited, and there are a number of constants that need to be determined from data analysis, it is not feasible to conduct full-blown calibration analysis. Rather, efforts were made in this study to compare the punchout information in actual pavement in Texas with the predictions from MEPDG. Unfortunately, using national calibration constants for the punchout model resulted in far more punchouts than observed in actual CRCP in Texas. In addition, it turned out that the two actual punchouts used for the comparison actually did not follow the punchout mechanism assumed in MEPDG. The next chapter provides more detailed discussion on the probable mechanism for the two punchouts.

Chapter 4. Punchout Mechanism in CRCP in Texas

In order to develop an accurate punchout prediction model, it is essential to understand the exact mechanism for punchout. It takes quite a while for punchout to develop and it's not easy to observe the progress of punchout in the actual pavement, because once punchout occurs it is repaired rather quickly. In addition, it has been observed in the field during the course of this and other TxDOT research projects that there are different distresses that are currently identified as "punchout." This chapter discusses various distresses in CRCP observed in Texas and provides probable mechanisms for those distresses, and suggests further research needed to refine or improve current punchout prediction models.

4.1 Distresses in CRCP in Texas

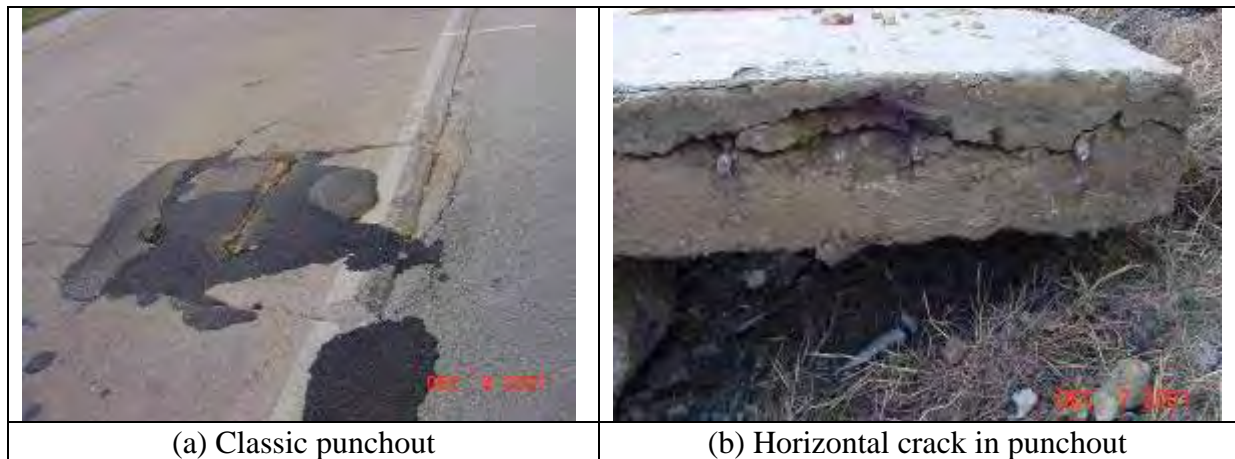
TxDOT's current "Pavement Management Information System—Rater's Manual" (PMIS) (9) identifies five distress types in CRCP: spalled cracks, punchouts, asphalt patches, concrete patches, and average crack spacing. In this classification system, punchout is the only un-repaired structural distress and both asphalt and concrete patches are assumed to have been done to repair punchouts. In other words, except for spalled cracks and average crack spacing, all the other distresses and repairs are related to "punchouts." The Manual provides three example pictures for punchouts as shown in Figure 4.1. Even though all the three distresses shown in Figure 4.1 may meet the definition of punchouts, their development mechanisms may not be the same, and as a matter of fact, their mechanisms could be quite different as will be discussed later. For example, the second and third pictures shown in Figure 4.1 have to do with concrete material quality and design/construction quality than structural deficiency in CRCP. In CRCP, punchout is considered as a distress caused by deficiencies in the structural capacity of the pavement system. Therefore, when distresses identified as punchouts are excessive in CRCP, it is assumed that the pavement system, or more often, the slab thickness was deficient for the given truck traffic. The consequence of this kind of logic is that, if misdiagnosis is made in identifying punchout, pavement design could become more conservative than needed. Considering the current fiscal constraints each state DOT, including TxDOT, is experiencing, improper or incorrect identification of punchout in CRCP has significant consequences in DOT operations. In this section, detailed discussions are presented along with actual distresses observed in Texas on the potential mechanisms and what could be done to prevent or minimize those distresses. It is expected that understanding correct distress mechanisms would help enhance the accuracy of TxDOT's pavement design procedures, which will ultimately result in more efficient use of financial resources to better address the needs of pavement system in TxDOT. In this section, distresses observed in Texas that are currently identified as punchouts are discussed in detail. Possible distress mechanisms are presented. Because CRCP has not been used in other states as extensively as in Texas, most of the national research efforts in Portland cement concrete (PCC) have been devoted to jointed concrete pavement (JCP). Consequently, not much national research effort has been made in CRCP. Fortunately, over the years TxDOT has sponsored a number of research projects on CRCP, including this rigid pavement database project, and a substantial amount of information has been gathered on CRCP structural responses and performance. This section discusses distresses observed in CRCP in Texas, and their potential mechanisms are presented based on the information obtained and knowledge gained through the research projects sponsored by TxDOT.



Figure 4.1: Examples of punchout in TxDOT PMIS Rater's Manual

4.1.2 Distresses due to Horizontal Cracking

Before the discussion of distresses in CRCP, it should be noted that most of the CRCP sections in Texas that exhibit distresses served much more than intended design lives. The section discussed in the previous chapter is a good example. Even though the design life of the section was 20 years, it still provides good performance after 38 years of service, which means almost double the design life in terms of time. In terms of traffic, it could be more than double. In other words, even though CRCP sections might experience distresses, it does not mean that the sections were under-designed. Rather, we are observing distresses because the CRCP carried traffic and environmental loading far beyond its intended capacity. Figure 4.2-(a) shows a classic example of edge punchout. This pavement on IH 35W in the Dallas District—8-in. CRCP over cement-treated subgrade—was built in 1966 and served well for more than 35 years when the District decided to place asphalt overlay.



(a) Classic punchout

(b) Horizontal crack in punchout

Figure 4.2: Punchout and horizontal cracking

It is shown that there is evidence of pumping and subsidence of asphalt shoulder and concrete pavement edge. This distress appears to have followed the punchout mechanism in MEPDG; however, distressed concrete slab removed in this area shows evidence of horizontal cracking at the depth of longitudinal steel as shown in Figure 4.2-(b). It appears that the punchout in this case followed a mechanism that has not been fully understood. Another

evidence of distress due to horizontal cracking is shown in Figure 4.3. This pavement on US 287 in the Wichita Falls District (the section evaluated for calibration of MEPDG as discussed in the previous chapter, 8-in. CRCP over asphalt stabilized subbase) was built in 1970. This distress was first observed by the research team in August 2005. Since then, periodic evaluations were made along with coring on November 16, 2007.

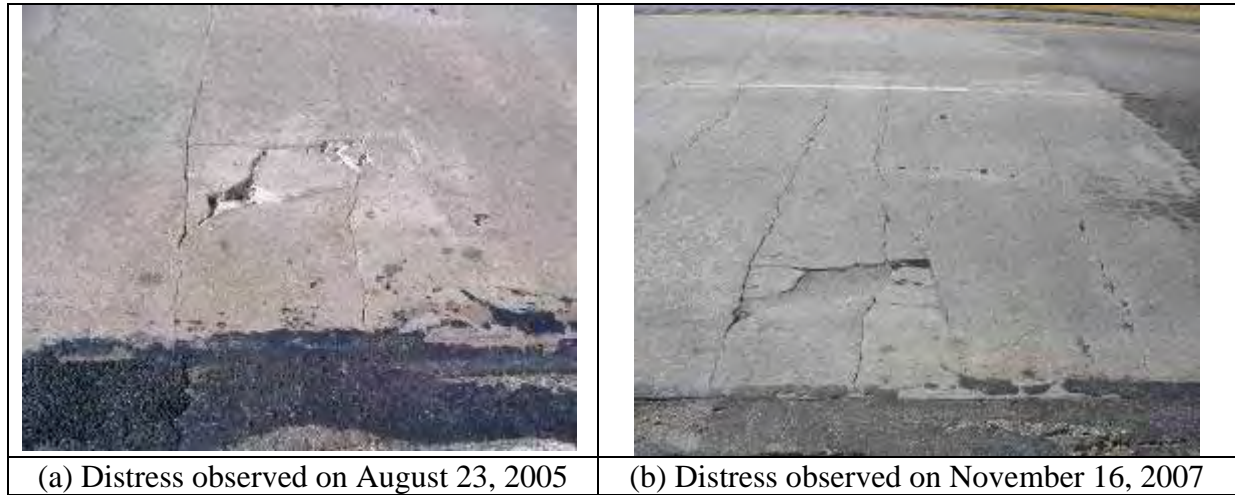


Figure 4.3: Distresses observed

Figure 4.3-(a) shows the distress observed on August 23, 2005. As discussed in the previous chapter, this section has average annual daily traffic (AADT) of 16,350 with 34% trucks. Two longitudinal cracks are observed along with a short transverse crack within a block bounded by two longitudinal cracks. It is also noted that transverse cracks near the slab edge are in better condition than those inside of the slab. This is important because the punchout model in MEPDG assumes that transverse cracks will deteriorate near the pavement edge, which will result in top-down longitudinal cracks 4 ft away from the pavement edge and eventual punchout. Figure 4.3-(b) shows the distress observed on November 16, 2007. Asphalt materials were applied and deterioration of concrete extended to the area with narrow transverse crack spacing. On the other hand, transverse cracks at pavement edge are still in good condition.

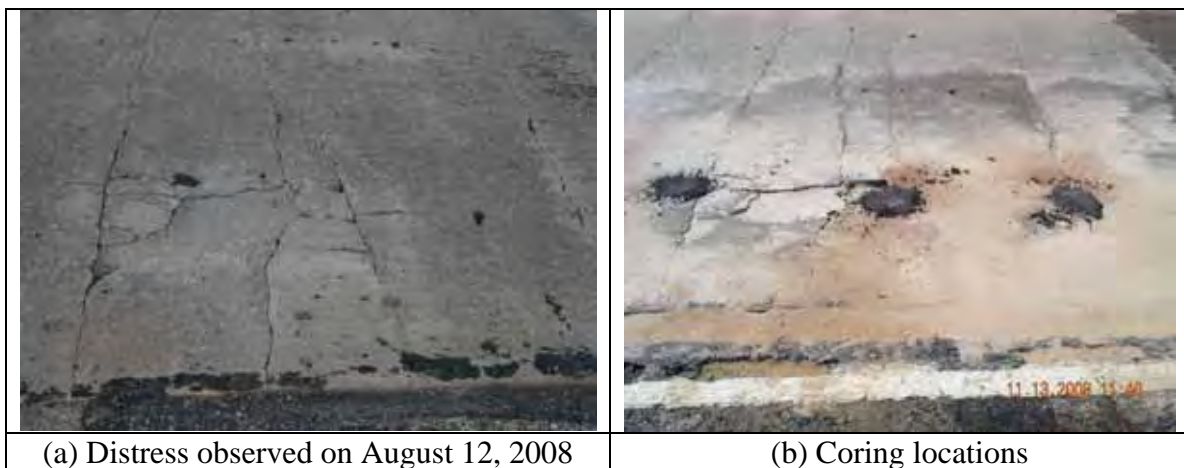


Figure 4.4: Distress at coring locations

Figure 4.4-(a) shows the pavement condition observed on August 12, 2008. Compared with Figure 4.3-(b), longitudinal cracks started forming from two transverse cracks. It is also noted that transverse cracks at the edge of the pavement were still in good condition. To fully understand the condition of concrete pavement, coring was conducted on November 13, 2008. A total of 3 cores were taken as shown in Figure 4.4-(b). The three core locations were 32 inches transversely from the pavement edge. Figure 4.5-(a) shows a core taken at the far left in Figure 4.4-(b). It is noted that the longitudinal crack formed along the longitudinal steel. Also noted is that, even though the longitudinal crack was quite tight on the surface, the crack was full-depth. However, it was not feasible to determine whether it was top-down or bottom-up cracking. It could be that the longitudinal crack formed by the interactions between concrete and steel in response to dynamic traffic loading. Figure 4.5-(b) shows a core taken in the middle shown in Figure 4.4-(b). Severe horizontal cracking is noted. On the other hand, compared with the distress in the upper part of the core, the bottom concrete below the longitudinal steel appears to be in good condition. Also observed is that the longitudinal crack was along the longitudinal steel.

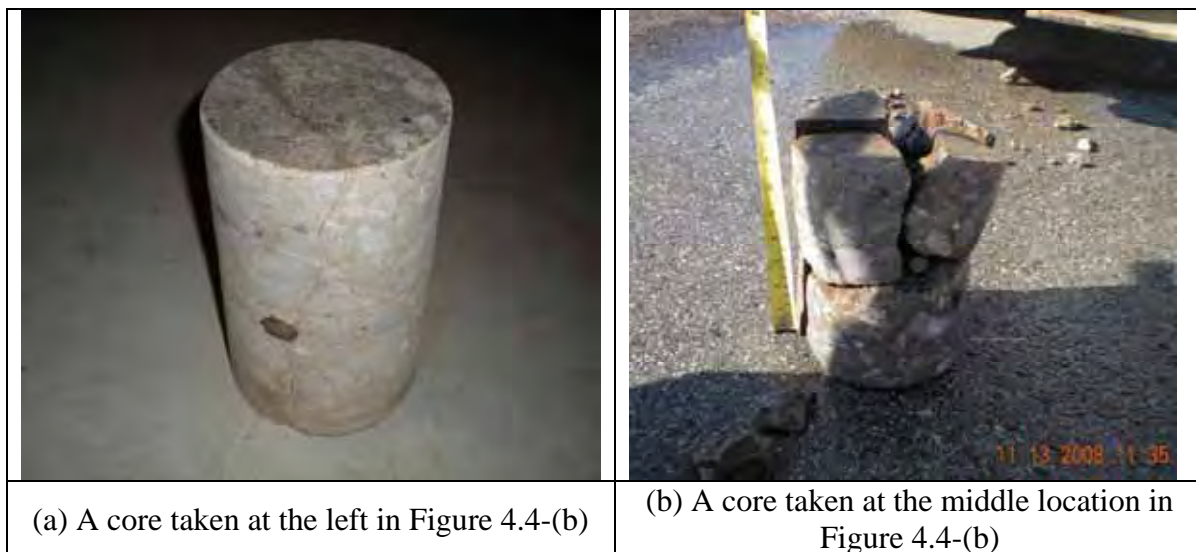


Figure 4.5: Condition of cores taken

Figure 4.6-(a) shows a fine longitudinal crack that formed on one side of the transverse crack. A core was taken from this location, which is the far right in Figure 4.4-(b). The core taken is shown in Figure 4.6-(b). It is noted that the longitudinal crack is along the longitudinal steel and evidence of horizontal crack at the depth of longitudinal steel. The observation of the progress of deterioration in this area reveals the following:

- (1) Longitudinal cracks formed over longitudinal steel. It appears that longitudinal cracking was not top-down or bottom-up cracking due to wheel loading applied at the pavement edge. Rather, it appears that longitudinal cracking could have been due to the interactions between concrete and steel in response to dynamic traffic loading.
- (2) Early signs of horizontal cracking were observed at the depth of longitudinal steel.
- (3) The severe distress observed in the surface is due to horizontal cracking at the depth of longitudinal steel, even though the bottom concrete appeared to be in good condition.

(4) It is interesting that, even though asphalt shoulder was used, transverse cracks at the pavement edge in the deteriorated area appeared to be tighter than the cracks in the inside the slab. This indicates that the punchout mechanism in MEPDG, narrow crack spacing and large crack width, along with degraded LTE and loss of support causing top-down longitudinal cracking and punchout, may not apply to this distress.

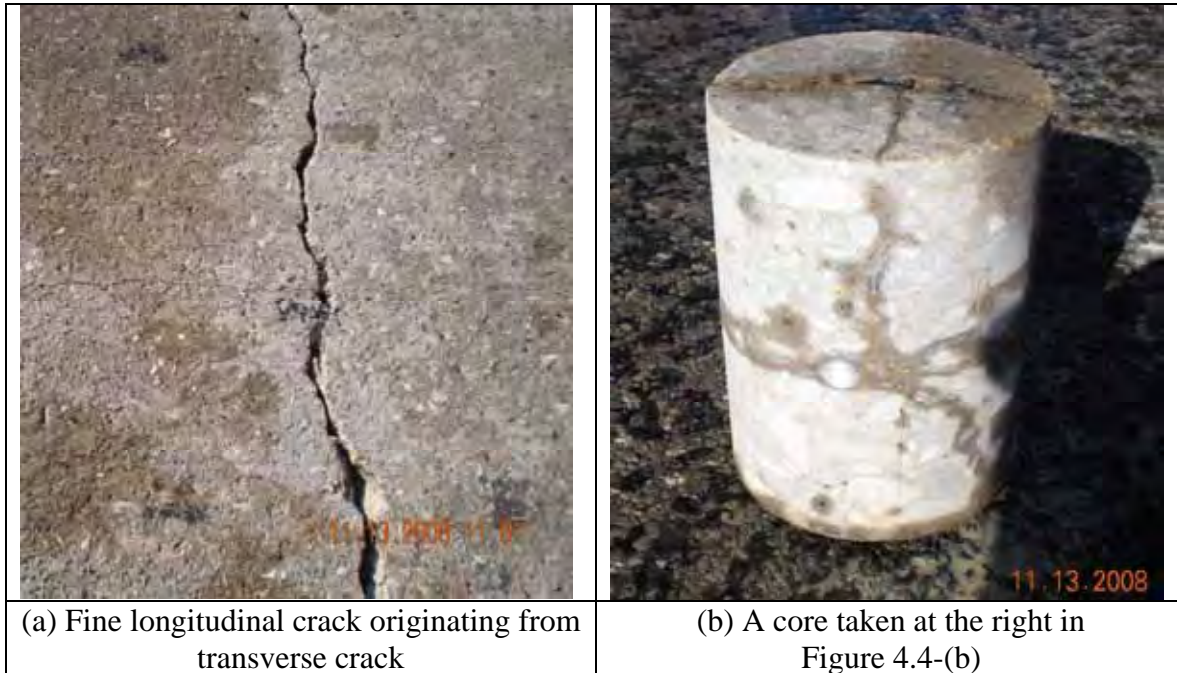


Figure 4.6: Longitudinal cracking and sample core

A 3-mile section of US 281 in the Wichita Falls District, which was built in early 1960s, experienced severe distresses as shown in Figure 4.7-(a). The slab is 8 in. on top of prepared subgrade. The section was rehabilitated with 4-in. bonded overlay in June 2002, and prior to the overlay, full-depth repairs were conducted. Figure 4.7-(b) shows the slab taken out during the full-depth repair.



Figure 4.7: Distresses in US 281

All the longitudinal cracks were along the longitudinal steel. Also noted are horizontal cracks, some of which are at the depth of longitudinal steel, and some of which are closer to the bottom of the slab. The coarse aggregate used was crushed limestone, which normally has low coefficient of thermal expansion (CoTE) and modulus of elasticity. Thanks to these desirable concrete properties containing crushed limestone, CRCP sections with crushed limestone rarely show horizontal cracking due to environmental loading at early ages. It appears that the horizontal cracking in this section was due to the interactions between concrete and longitudinal steel in response to truck traffic applications.

Longitudinal cracking and associated distresses were observed on IH 30 in the Paris District. The pavement consists of 10-in. CRCP over 4-in. asphalt subbase on top of old jointed concrete pavement. Therefore, this section is classified as unbonded overlay. This pavement section was built in the middle of 1980s. Figure 4.8-(a) shows a typical distress observed in that section. It is noted that longitudinal cracking developed between two closely spaced transverse cracks. Figure 4.8-(b) shows the slab segment taken out from the distressed area on the same highway, but not from the area shown in Figure 4.8-(a). Longitudinal cracks developed along the longitudinal steel and horizontal cracking is observed at the depth of longitudinal steel.

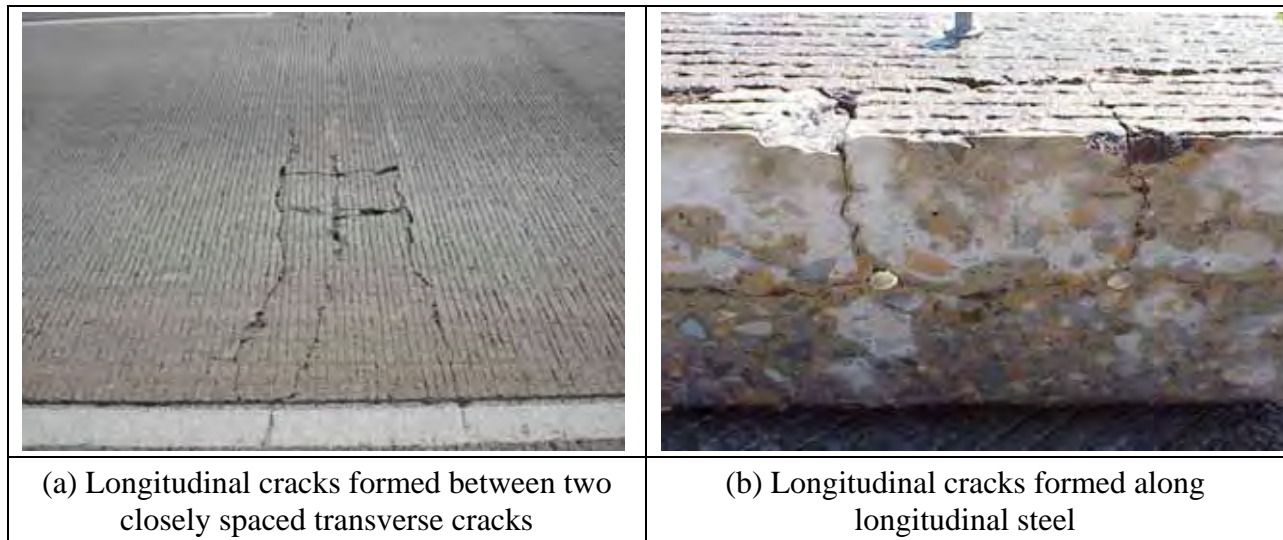


Figure 4.8: Longitudinal and horizontal cracks

Longitudinal cracking was observed on US 290 eastbound just south of Hempstead. This section was constructed in 1995, and the pavement structure consists of 10-in. concrete slab+1-in. asphalt bondbreaker+6-in. cement stabilized subbase+6-in. lime treated subgrade. Figure 4.9-(a) shows a longitudinal crack, which was 14-in. from the intended longitudinal warping joint. The saw-cut depth at the warping joint was insufficient and no crack was developed under the saw-cut as of January 2009. Instead, longitudinal cracks formed near the warping joint. Figure 4.9-(b) shows a core taken at the longitudinal crack. It is shown that the longitudinal crack was along the longitudinal steel. However, horizontal cracking is not noted. Based on the observations on the distresses in CRCP in Texas, it is postulated that horizontal cracking might eventually form in this section once additional transverse cracks form due to fatigue, which will be discussed in the next section. Figure 4.10-(a) shows a quite fine longitudinal crack formed on the same US 290 section. Compared with the transverse crack shown in the picture, the longitudinal crack is so tight that it looks as though it just started forming. A core was taken at the location marked, and Figure 4.10-(b) shows that longitudinal crack was along longitudinal steel, as in the previous cases, and actually quite wide within the slab, even though the crack was so tight on the surface. This implies that the longitudinal crack might not be due to the mechanism of top-down or bottom-up cracking; rather, it could be that the interactions between concrete and longitudinal steel during wheel loading applications could have caused this longitudinal crack.



Figure 4.9: Longitudinal cracking on steel

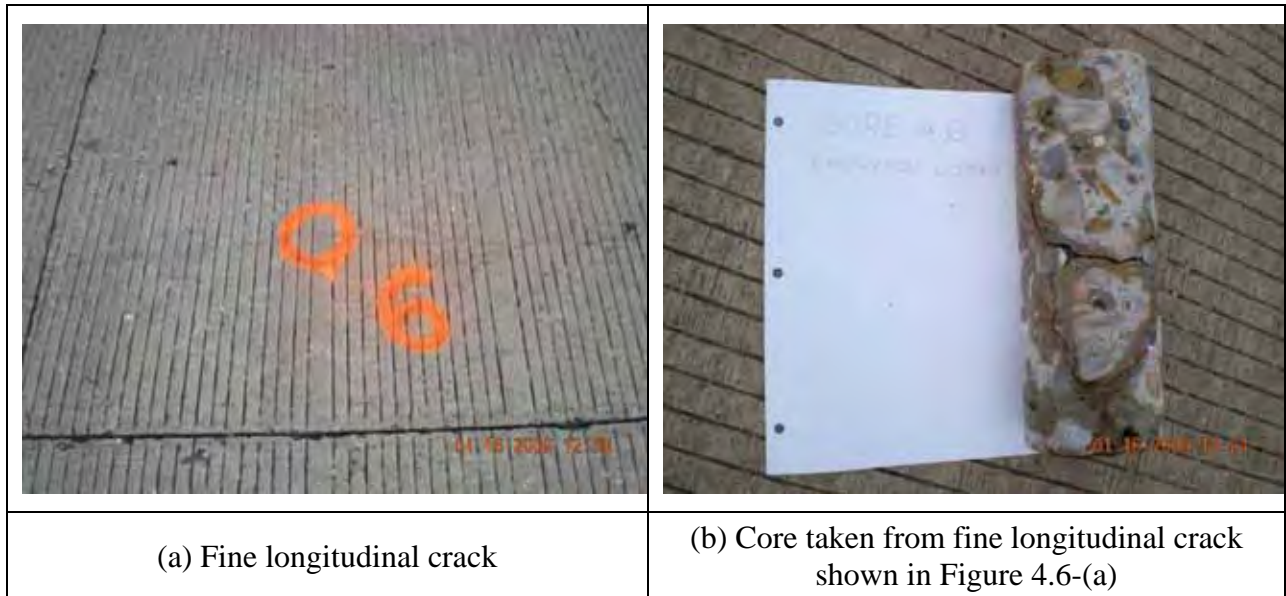


Figure 4.10: Fine longitudinal cracks

Observations of full-depth repair projects in CRCP revealed that most of the distresses, if not all, were due to horizontal cracking at the depth of the longitudinal steel. Not much research has been done on horizontal cracking. Currently, there is a TxDOT research project underway on horizontal cracking (0-5549), and the major focus of that study is how to mitigate horizontal cracking that forms at the early age due to temperature and moisture variations in concrete. When the 0-5549 project was initiated, the extent of horizontal cracking in old CRCP and its association with what appeared to be full-depth punchout were not well understood. Instead, horizontal cracking was observed in brand new CRCP on IH 35 in Waco even before the pavement was open to traffic. Due to the lack of complete understanding of the horizontal cracking in CRCP at that time, the scope of the current 0-5549 was confined to early-age aspect of horizontal cracking. Based on the observations made in this database and other TxDOT projects, it appears that horizontal cracking that develops in old CRCP due to traffic loading

applications is an essential element of CRCP distress mechanism. This aspect is currently under investigation in TxDOT's research study 0-5832, where efforts are being made to develop improved mechanistic-empirical CRCP design procedures.

4.1.3 Fatigue Cracking

During the field evaluations of old CRCP condition in Texas, it was discovered that transverse fatigue cracking started forming in slab segments with relatively large crack spacing. Transverse cracking that forms at early ages due to temperature and moisture variations has quite uniform crack width from one end of the crack to the other end through the slab width. Later, abrasion loss of cement hydration products from pavement surface due to wheel loading applications makes the crack widths look wider on the surface, especially near the wheel path. However, crack widths near the pavement edge remain quite tight, unless subbase erosion and resulting pumping exists, in which case the opposite takes place, i.e., crack widths are larger near the pavement edge. Figure 4.11 shows a typical crack width variation near the pavement edge. Note quite tight crack widths near the pavement edge in the two transverse cracks that run all the way through the slab width, while inside the slab, crack widths look rather large.

In Figure 4.11, a transverse crack is shown in between two transverse cracks. The section shown here is in US 287 section discussed in Chapter 3. This picture was taken in January 2009, so this pavement was more than 38 years old. The width of this crack at the pavement edge is larger than the widths of the other two transverse cracks. There were a number of transverse cracks that formed between two transverse cracks that run through the whole slab widths. These cracks appear to have formed rather recently, because they look tighter than adjacent cracks and started at the pavement edge and are progressing towards the inside of the slab. Because the stress due to wheel loading is quite large when it is applied near slab edge, especially when asphalt shoulder is used, it is believed that these cracks were formed due to the fatigue of concrete from repeated wheel loading applications near the slab edge.



Figure 4.11: Transverse fatigue crack formed between two old transverse cracks

This finding is quite significant in understanding how CRCP punchouts form. While the wheel loading applications induce new transverse cracks, they did not deteriorate the condition of existing transverse cracks. In other words, the premise made in traditional punchout models—wheel load applications deteriorate aggregate interlock at transverse cracks, which reduces LTE, increases concrete stress in transverse direction at the top of the slab, and eventually causes punchouts—may not be valid in all situations. Figure 4.12-(a) shows another transverse fatigue crack in US 287 section discussed in Chapter 3. It shows that this transverse crack is in between two transverse cracks, which extended all the way through the pavement width, started from pavement edge and were extending towards the inside of the slab. There was a longitudinal crack at the location marked by red circle. A core was taken at that location and is shown in Figure 4.12-(b). As in the previous cases, the longitudinal crack was along longitudinal steel and there is horizontal cracking.

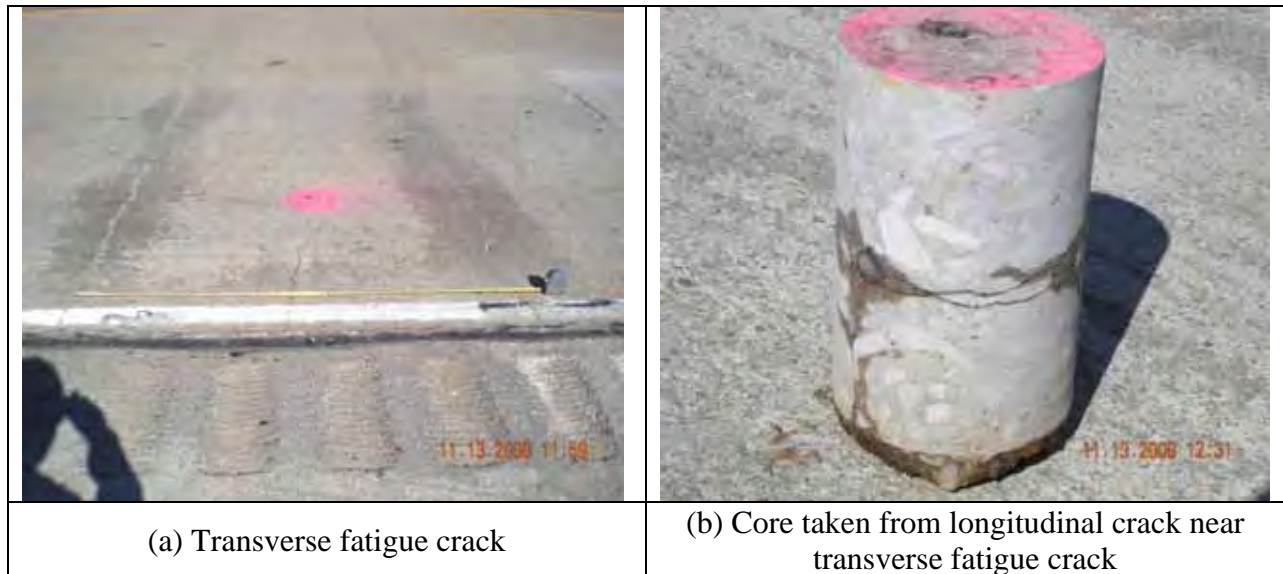


Figure 4.12: Transverse fatigue crack

It is postulated that, eventually, horizontal cracking will extend and cause deterioration on the upper half of the slab above the longitudinal steel.

4.1.4 Other Distress Types

Figure 4.13-(a) shows disintegration of surface concrete near the warping joint. This pavement section is located on US 75 in the Paris District. The coarse aggregate type used is sandstone from Oklahoma. The CoTE value of this material is quite high, exceeding 6 microstrains per F. This distress resembles the third punchout example in TxDOT PMIS Rater's Manual as shown in Figure 4.1. Because the bottom concrete is in sound condition, it appears that this distress was not caused by the structural deficiency of the pavement system. Rather, it appears that the concrete material properties, the quality of construction, and/or environmental condition during and immediately after the construction could have caused this distress. This type of distress also appears to be related to the location of longitudinal steel. The closer the location of the longitudinal steel to the slab surface, the higher the probability of this type of crack. Theoretical analysis conducted under TxDOT research study 0-5549 (horizontal cracking) confirms the effect of the depth of longitudinal steel on this type of distress. Because this distress is not due to structural deficiency of CRCP, it should not be classified as punchout.

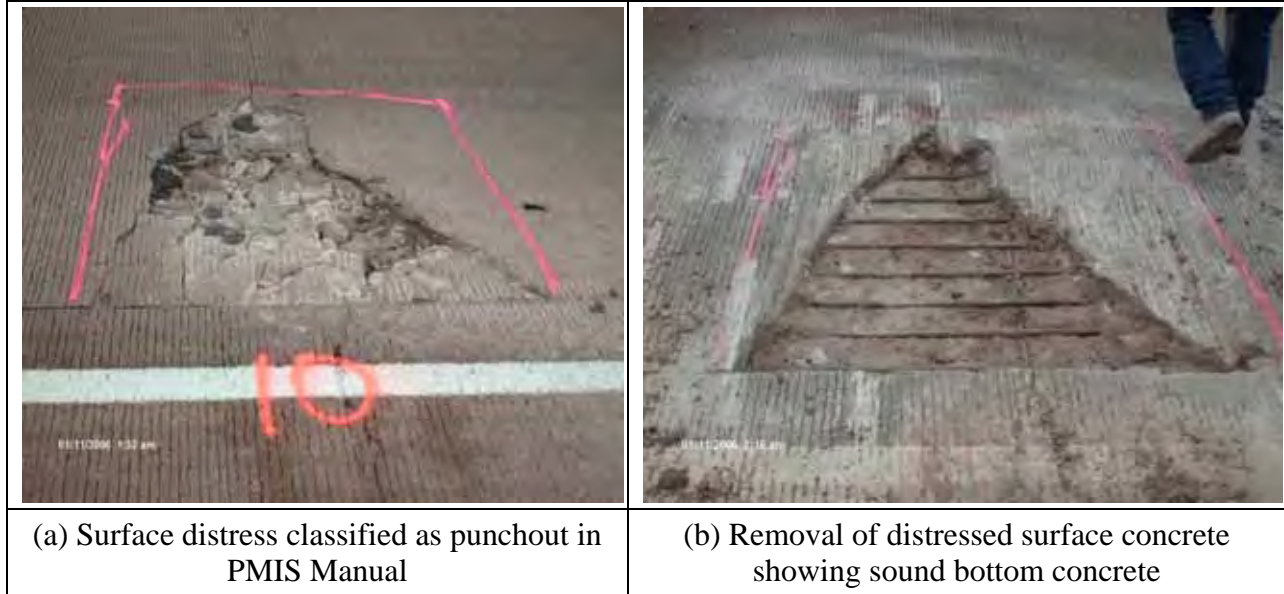


Figure 4.13: Surface distress

Figure 4.14-(a) shows a typical distress observed at the perimeter of the previously repaired area. This distress resembles the second punchout example in TxDOT PMIS Rater's Manual as shown in Figure 4.1. Figure 4.14-(b) also shows similar distress next to transverse construction joint. These two distresses are not due to structural deficiency of CRCP system; rather, they are due to imperfections in design details and/or material/construction deficiencies. These distresses should not be classified as punchouts.

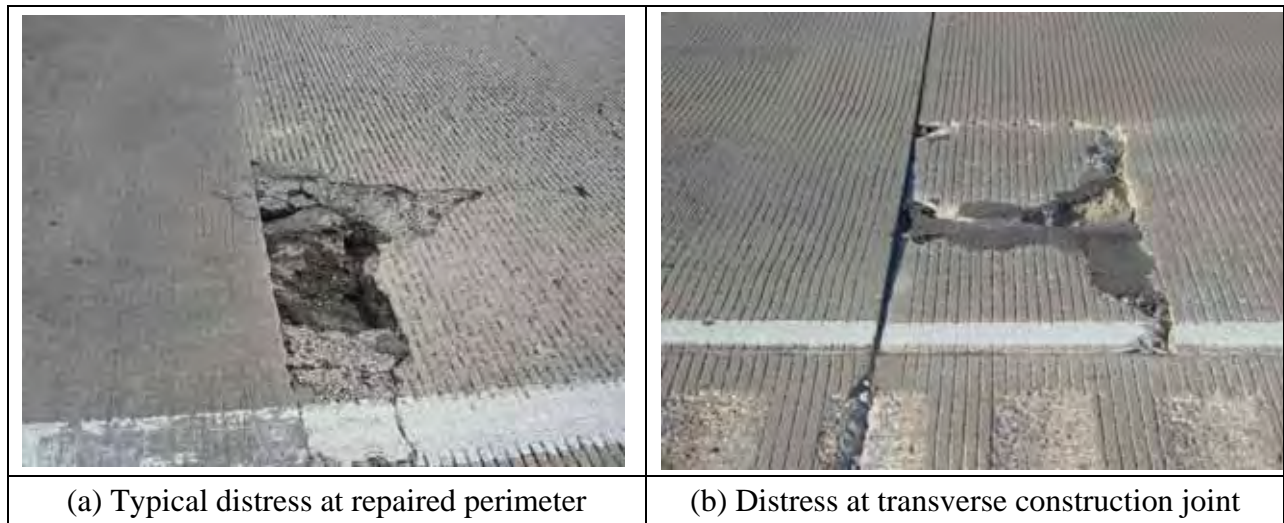


Figure 4.14: Distress at perimeter and joint

4.2 Discussion

In this chapter, typical CRCP distresses observed in Texas were presented along with probable mechanisms. It has been shown that many distresses identified and recorded as punchout in TxDOT's PMIS might not be true punchout. Rather, most of them are more related to imperfections in design details and/or construction/materials quality. In other words, the number of punchouts in TxDOT's PMIS might be over-estimated.

It has been observed that most of the distresses that required full-depth repair in CRCP, if not all, were related to horizontal cracking. Horizontal cracking appears to be caused by the interactions between longitudinal steel and concrete in response to repeated truck traffic loading applications. This aspect of the distress has not been addressed up to now. Efforts are underway to investigate the mechanism of this distress in TxDOT research study 0-5832.

Based on the findings in this project, it appears that punchout mechanism should be re-evaluated for its validity. Identifying correct punchout mechanism and collecting valid punchout field data is essential to improving CRCP design procedures. Also, it appears that the punchout portion of Rater's Manual needs to be revised; developing a training manual for the correct identification of punchout as well as recording other types of CRCP distress could help improve TxDOT's PMIS.

Chapter 5. Manual for Database Administrator

This chapter presents the manual for administrator of the rigid pavement database (RPDB) developed in this project. Detailed description of the RPDB is included in the companion product (P2) of this project, “Manual for Web-based TxDOT Rigid Pavement Database.” There are three levels of accounts provided in RPDB: (1) Server Manager or Administrator, (2) Webpage Developer, and (3) User. This chapter provides a manual for the RPDB Administrator only.

The RPDB currently resides in MapServer at the Center for Geospatial Technology at Texas Tech University. RPDB can be accessed at the following URL:

<http://mapserver.gis.ttu.edu/txtechdot>

5.1 RPDB Contents

The RPDB involves three types of data input files:

- A. General Pavement Section Information
- B. Detailed Pavement Section Testing Data
- C. On-site Pictorial Presentation for Each Test Section

5.1.1 General Pavement Section Information

- These files contain all the basic information necessary to geographically identify a particular pavement section.
- The GPS start and end coordinates provided are essential for plotting the particular pavement section onto a base map of the State of Texas using the ArcGIS software ArcMap. This base map along with the plotted test sections are then shared onto a server and used to develop a user-interactive web-service. Thus, this information is pivotal in providing the input for the Web-Based Information System.
- This data is presented in Microsoft Excel or Microsoft Access formats in order to be readily compatible with the current ArcGIS software (ArcMap 9.3 and ArcGIS Server 9.3).
- This data also includes the Test Section ID, District Name, County Name, Direction, Reference Marker, Pavement Type, number of lanes, etc., so as to enable identifying a particular test section by querying the desired criteria.
- The file containing the test section data should be named as per the Test Section ID for easy identification.

5.1.2 Detailed Pavement Section Testing Data

- These files contain information on the structural responses of the pavement test sections and condition information. The data includes transverse crack spacing, falling weight deflectometer (FWD) deflections, and load transfer efficiency (LTE).

- All pavement testing data files are stored in Microsoft Excel 2007 or Microsoft Access 2007 format for uniformity and easy access to the users.
- A separate file for each testing data is created and named according to the Section ID and the type of test data in order to enable query-based analysis. These files are stored in a common folder containing data for the corresponding road section.

5.1.3 On-site Pictorial Presentation for Each Test Section

- These files provide the actual graphical images of the pavement sections.
- These files should be present in JPEG, GIF, PNG, or TIFF formats.
- Similar to all other file types, these files should be labeled in accordance with the Section ID because the query analysis uses Section ID and picture number as the key.
- The picture folder for each section should be stored in a folder labeled with the test Section ID and stored in the base folder containing all the detailed data for that particular section.

For the presently developed web-application, the following names for files are used:

1. General Pavement Section Information: *GI_”Section I.D”*
2. Detailed Pavement Section Testing Data:
 - For FWD Data: *FWD_”Section ID”*
 - For LTE Data: *LTE_”Section ID”*

All the data files for a particular pavement section are stored in the same folder named according to its corresponding Section ID.

5.2 Internal Structure of RPDB

Figure 5.1 illustrates the internal structure of the RPDB along with the interactions among various components in the RPDB. The pavement test section data as well as the GIS data need to be shared over a server in order to effectively update the data, develop the web-application, reflect changes in the data within the web-application, and assure ease of access to the Administrator and Webpage Developer as well as the end user. The server also needs to have a domain so that the application that is accessed over a network can call the data from the server. The space required on the server to store the database depends on the size of the database as well as on how user-interactive and graphically rich the web-application needs to be.

For the presently developed web-application, the MapServer at the Center for Geospatial Technology at Texas Tech University is used to host the database and develop the application. For developing the application, ArcGIS Server software is installed on the server being used to share the data and, using ArcGIS Server Manager, the web-based interface is developed. The Map document stored as an .mxd file, the GIS data in the folder “*Data*,” and the pavement section data in the folder “*Web*” are shared over the MapServer.

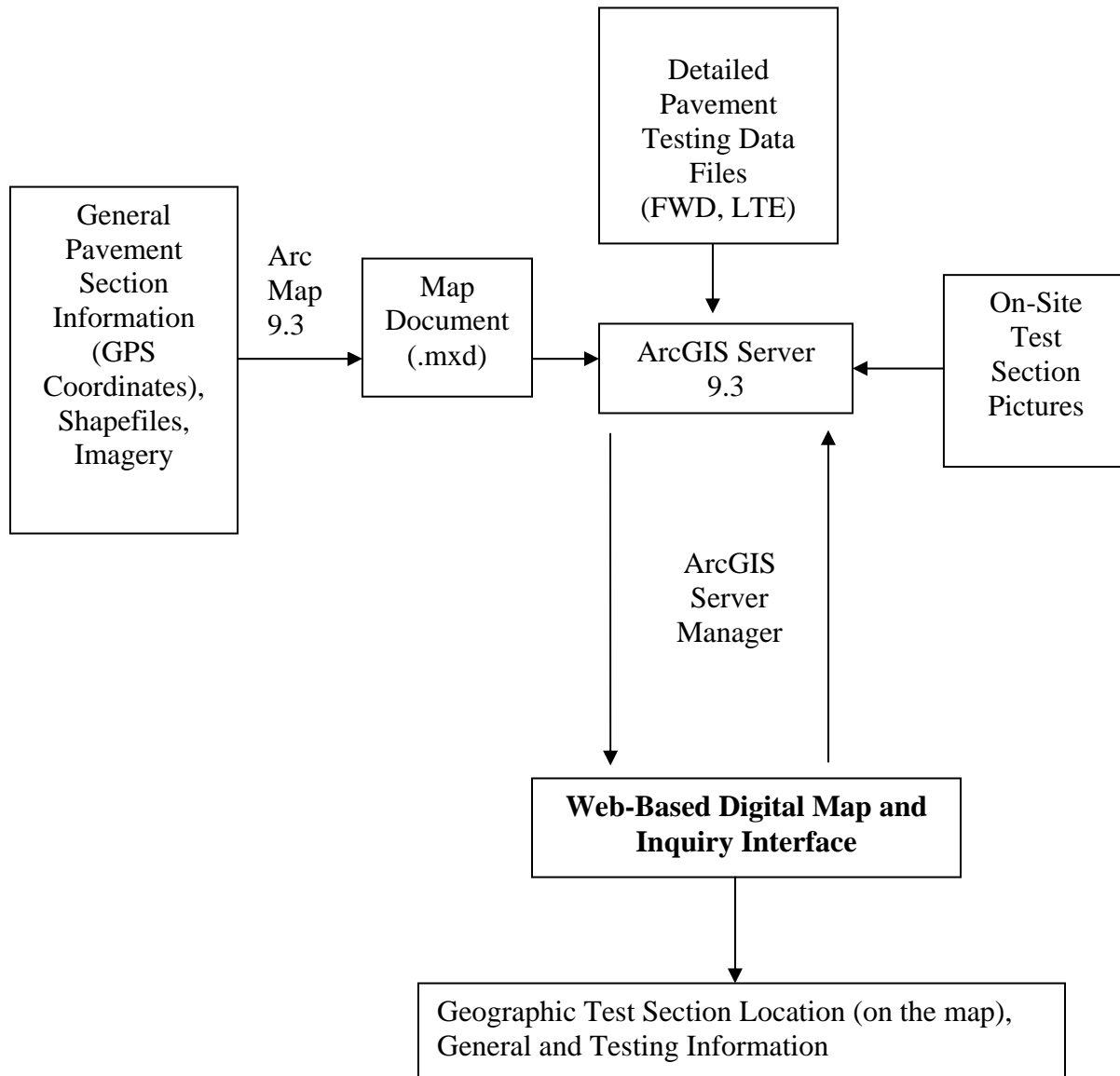


Figure 5.1: RPDB internal structure diagram

5.3 Development of the Web-Application

The web-application that provides a user-interactive interface for accessing the pavement test data and making a query-based analysis is developed in a two-step process. This process involves first developing a map document with all the geographic attributes using ArcMap and then sharing the data and developing the web-application using ArcGIS Server.

5.3.1 Developing the Map Document

- The Map document developed for the web-application using ArcMap contains different shapefiles for the county boundaries (*Counties*) and imagery files for the counties as well as the road layers for the different counties across the state. Figure 5.2 shows a graphical illustration of map document.

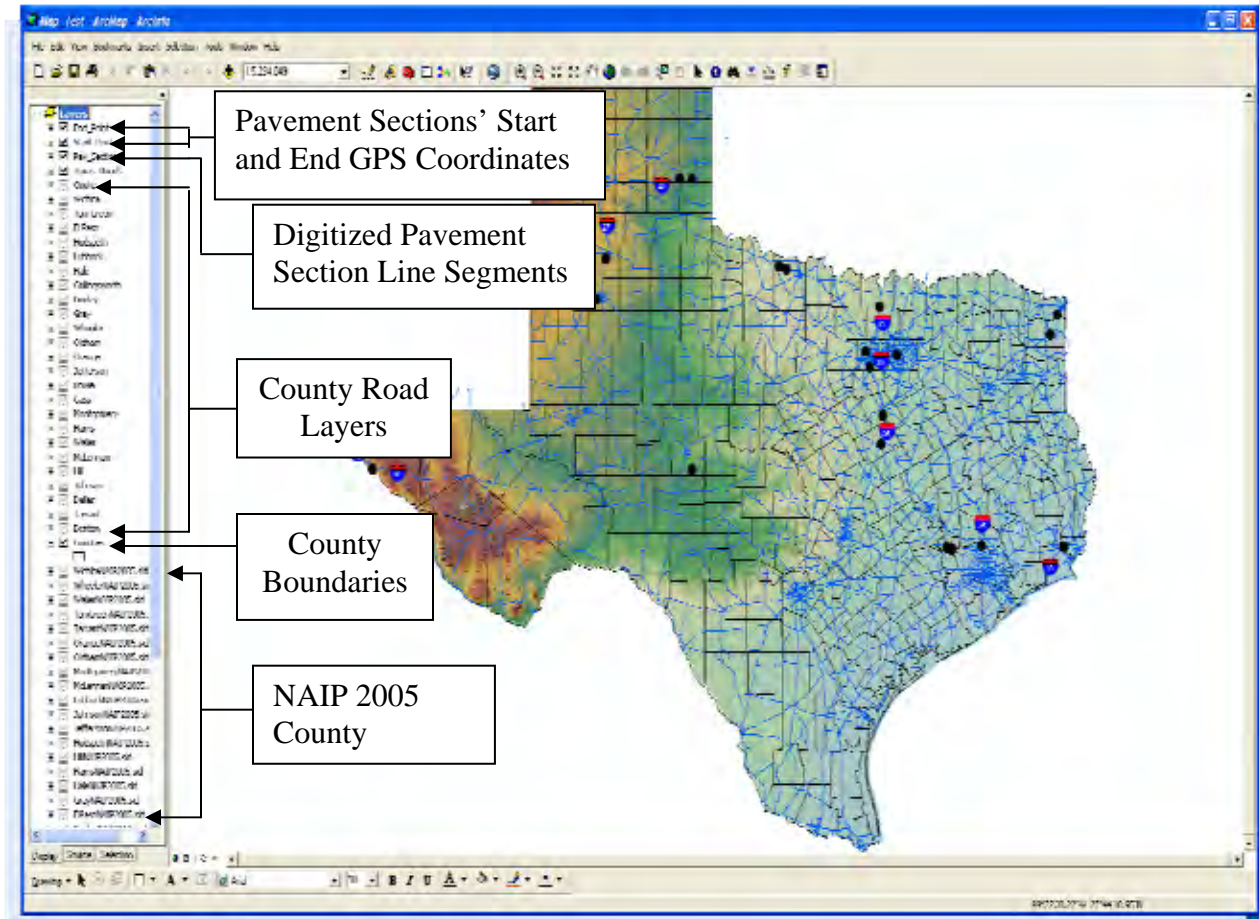


Figure 5.2: Map Document

- All shapefiles and image files are directly added to the Map document from their respective folders on the server using the *Add Data* Tool.
- The GPS Coordinates for the start and end points of the pavement test sections are stored in an Excel sheet on the sever and these can be directly added to the Map Document using the tool *Add X-Y Coordinates* in ArcMap.
- For connecting the end points of the test sections, a shapefile called *Pav_Sections* is first created in Arc Catalog and consecutively added to the map document. Thereafter, using the *Editor* Toolbar in ArcMap, each pair of end points is graphically joined and when these changes are saved, a digitized layer containing the pavement test sections is created.

- The attribute table for the *Pav_Sections* shapefile is added with a field that specifies the Section ID for each test section and also with fields for the general information as well as test results. The General Information and Test Result fields specify the path wherein the corresponding files for the test sections are stored on the server. Figure 5.3 shows attributes of pavement sections.

ID	Shape	SECTION ID	Gen. Info	File	LTE
0	Pavline	0 507-1	507-10_507-1.shp	507-1\FMD_507-1.shp	507-1\LTE_507-1.shp
1	Pavline	0 5-F288-1	542288-10_542288-1.shp	542288-1\FMD_542288-1.shp	542288-1\LTE_542288-1.shp
2	Pavline	0 2540-1	2540-10_2540-1.shp	2540-1\FMD_2540-1.shp	2540-1\LTE_2540-1.shp
3	Pavline	0 2440-1	2440-10_2440-1.shp	2440-1\FMD_2440-1.shp	2440-1\LTE_2440-1.shp
4	Pavline	0 2410-2	2410-20_2410-2.shp	2410-2\FMD_2410-2.shp	2410-2\LTE_2410-2.shp
5	Pavline	0 2410-3	2410-30_2410-3.shp	2410-3\FMD_2410-3.shp	2410-3\LTE_2410-3.shp
6	Pavline	0 2410-4	2410-40_2410-4.shp	2410-4\FMD_2410-4.shp	2410-4\LTE_2410-4.shp
7	Pavline	0 340387-1	340387-10_340387-1.shp	340387-1\FMD_340387-1.shp	340387-1\LTE_340387-1.shp
8	Pavline	0 340387-2	340387-20_340387-2.shp	340387-2\FMD_340387-2.shp	340387-2\LTE_340387-2.shp
9	Pavline	0 3405-1	3405-10_3405-1.shp	3405-1\FMD_3405-1.shp	3405-1\LTE_3405-1.shp
10	Pavline	0 2 800-1	2 800-10_2 800-1.shp	2 800-1\FMD_2 800-1.shp	2 800-1\LTE_2 800-1.shp
11	Pavline	0 18 00-1	18 00-10_18 00-1.shp	18 00-1\FMD_18 00-1.shp	18 00-1\LTE_18 00-1.shp
12	Pavline	0 2 05-1	2 05-10_2 05-1.shp	2 05-1\FMD_2 05-1.shp	2 05-1\LTE_2 05-1.shp
13	Pavline	0 3405-2	3405-20_3405-2.shp	3405-2\FMD_3405-2.shp	3405-2\LTE_3405-2.shp
14	Pavline	0 3405-3	3405-30_3405-3.shp	3405-3\FMD_3405-3.shp	3405-3\LTE_3405-3.shp
15	Pavline	0 1240280-4	1240280-40_1240280-4.shp	1240280-4\FMD_1240280-4.shp	1240280-4\LTE_1240280-4.shp
16	Pavline	0 1240280-2	1240280-20_1240280-2.shp	1240280-2\FMD_1240280-2.shp	1240280-2\LTE_1240280-2.shp
17	Pavline	0 1240280-3	1240280-30_1240280-3.shp	1240280-3\FMD_1240280-3.shp	1240280-3\LTE_1240280-3.shp
18	Pavline	0 12441-1-2	12441-1-20_12441-1-2.shp	12441-1-2\FMD_12441-1-2.shp	12441-1-2\LTE_12441-1-2.shp
19	Pavline	0 20410-1	20410-10_20410-1.shp	20410-1\FMD_20410-1.shp	20410-1\LTE_20410-1.shp
20	Pavline	0 194059-1	194059-10_194059-1.shp	194059-1\FMD_194059-1.shp	194059-1\LTE_194059-1.shp
21	Pavline	0 194059-2	194059-20_194059-2.shp	194059-2\FMD_194059-2.shp	194059-2\LTE_194059-2.shp
22	Pavline	0 440-1	440-10_440-1.shp	440-1\FMD_440-1.shp	440-1\LTE_440-1.shp

Figure 5.3: Attributes of Pavement Sections

- After the formation of the base map containing the counties and road layers, the process of adding the GPS coordinates of the end points and connecting the pavement sections is simplified by the previously described ArcMap tools.
- As a result, every time an update is made in the pavement database with the addition of a new pavement section and data related to it, the same can be introduced on the base map by the Account Administrator/Manager and will be consecutively reflected onto the web service.
- The map document is saved onto the server, in the same base folder where the *Data* and *Web* folders have been saved.

5.3.2 Authoring and Publishing a Map Service using ArcGIS Server Manager

- ArcGIS Server Manager is used to publish the web-application.
- To log into the ArcGIS Server Manager, the username and password of the server where all the data has been stored is required, as shown in Figure 5.4.



Figure 5.4: Logging in to ArcGIS Server Manager

- To begin creating a web-application, the first step involves using the *Create Web Application* tab on the ArcGIS Server Manager and specifying the name of the web application and general description.
- To publish the data stored on the server using ArcGIS Manager, a connection needs to be established to the specific server where the data is stored. This connection is created by using the *Add GIS Server* tab under the *Available Services List* box, typing the URL of the server and clicking *Add Server*.

As shown in Figure 5.5, from the drop-down list in the *Available Services* tab, the map document on the server that needs to be published is added to the *Selected Services*.

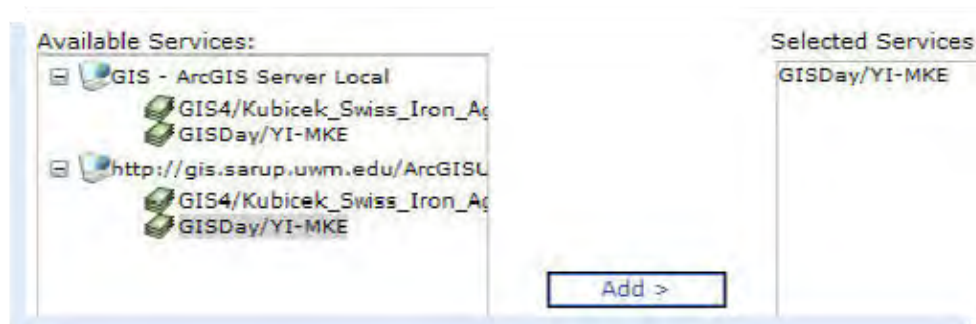


Figure 5.5: Adding the Map Document to the Web-Service

- The next panel prompt allows the user to select tasks for the web application to perform, to be added to the service as shown in Figure 5.6.

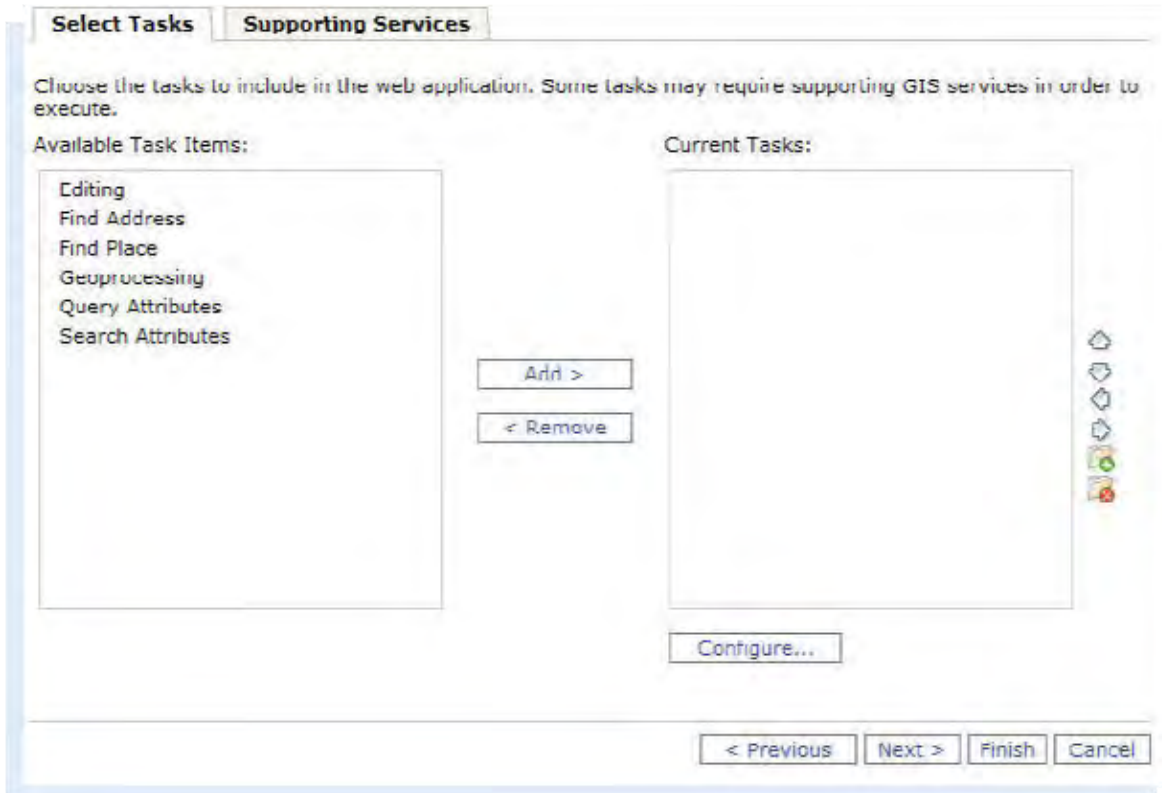


Figure 5.6: Selecting and Adding Tasks to the Map Service

- Through the *Supporting Services* tab, the attributes in each layer can be hyperlinked to a folder or file stored on the server. This is particularly essential in order to gain access to the pavement test section data from the website. The General Information, LTE and FWD data for each section is hyperlinked to their respective files stored on the server using this service.
- The title text and the theme of the webpage are added in the subsequent prompts.
- The *Enable Map Elements* prompt allows adding other features listed in Figure 5.7 to the map service. These features can be customized by the Web Developer using the *Settings* tab.



Figure 5.7: Adding Map Elements to the Map Service

- After adding the map elements, the Web Service is created in a separate window as prompted by the Developer.
- An important aspect that needs to be taken care of by the Server Manager/Administrator and the Webpage Developer is that every time data is updated on the server or a map document with changes is saved onto the server, the map service needs to be restarted from the ArcGIS Manager to reflect the changes onto the website.

Chapter 6. Summary and Recommendations

The mechanistic-empirical pavement design guide, called MEPDG, developed under NCHRP 1-37(A), presents the most advanced pavement design program developed so far. It incorporates the state-of-the-practice information and models to predict pavement responses and performance. For continuously reinforced concrete pavement (CRCP), based on the input values provided, it predicts crack width and load transfer efficiency (LTE), and concrete stress due to wheel loading applications. The wheel load stress is used to estimate the damages, and using a transfer function from damage to punchout, it predicts the number of punchouts for given traffic.

This algorithm deviates sharply from the current AASHTO pavement design guide, which was based on the AASHTO Road Test data and is much more empirical. One major difference, among others, between these two procedures is the inclusion of environmental effects in MEPDG, which could have significant implications, because pavement designers now have to consider when and where the pavement will be built. For the same project, pavement engineers might have to come up with several designs.

The findings from the work conducted in this research project can be summarized as follows:

- 1) Review of the punchout model in MEPDG
 - a) The punchout model in MEPDG is quite sophisticated, with a number of variables involved. It assumes that longitudinal crack is induced by top-down cracking.
 - b) The model is more applicable to CRCP with an asphalt shoulder. On the other hand, the model might not be appropriate for the punchout analysis of CRCP with tied-concrete shoulder.
 - c) Sensitivity analyses were conducted to investigate the effects of selected input variables on punchouts. Zero-stress temperature (ZST) had quite a large effect, primarily because crack width and LTE depend to a large extent on ZST.
 - d) There are three equations that can be calibrated using local information: (1) concrete fatigue, (2) damage-punchout transfer function, and (3) crack width. There are a total of six constants for these three equations. A number of CRCP sections with punchouts and accurate input values available are needed for calibration.
 - e) The MEPDG equation for crack width tends to over-predict crack width. Appropriate calibration constant needs to be determined.
- 2) Calibration of MEPDG Using Punchout Information
 - a) US 287 in Wichita Falls District was selected to compare the punchouts in actual CRCP with the predictions from MEPDG. The pavement section was built in 1970, with substantial truck traffic. After 38 years of service, two punchouts were observed in a 1.6-mile section, equivalent to 1.3 punchouts per mile. This section was selected for comparison with MEPDG predictions because this section has an

asphalt shoulder and has been in service for more than 38 years with heavy truck traffic.

- b) Efforts were made to determine reasonable values for major input variables. To determine ZST, actual crack spacing was compared with predicted values. The construction in March 1970 provided the closest average crack spacing to the actual value. It was assumed that the construction of this section was done in March, 1970.
 - c) The punchout estimate from MEPDG analysis with national calibration constants was 42.8 per mile. This value is much larger than the actual observed punchout.
 - d) Efforts were made to identify the cause for this large discrepancy. Because the MEPDG over-predicts crack width, smaller values for the calibration constant for crack width were used. If the value of 0.5 or less, the number of punchouts decreases to about 5. This value is still larger than the actual value, but much closer than the value with the national calibration constant for crack width.
 - e) Punchout prediction is not quite sensitive to the national calibration constants for the damage-punchout transfer function. For the CRCP section under evaluation, 10% deviation from the national constant resulted in 2 punchouts per mile.
 - f) Further efforts need to be made to collect more extensive punchout information.
- 3) CRCP Distresses in Texas
- a) It appears that many distresses identified and recorded as punchouts in Texas are not actually punchouts caused by structural deficiency. Rather, most of them are due to imperfections in design details and/or construction/materials quality issues.
 - b) Transverse fatigue cracking was observed that forms from the pavement edge, which implies that the critical stress is in longitudinal direction unless erosion and pumping exist.
 - c) Horizontal cracking appears to be the major cause for distresses in CRCP in Texas. The interactions between longitudinal steel and concrete in response to dynamic wheel loading applications appear to be the cause of horizontal cracking.
 - d) It is recommended that efforts should be made to accurately identify punchout during field evaluations. At this point, the punchout information in TxDOT's PMIS doesn't appear to be accurate.
 - e) It is also recommended that the punchout portion of the Rater's Manual needs to be revised.
- 4) Rigid Pavement Database Manual for Administrator
- a) Web-based and GIS-based rigid pavement database (RPDB) was developed in this study.
 - b) Detailed description of the RPDB is described in the companion product P2 of this project.
 - c) RPDB manual for administrator is included in this report.

References

1. ARA, Inc., ERES Division (2003) "Guide for Mechanistic-Empirical Design of New and Rehabilitated Pavement Structures," Final Report, Champaign, Illinois.
2. American Association of State Highway and Transportation Officials (1993), "AASHTO Guide for Design of Pavement Structures," American Association of State Highway and Transportation Officials, Washington, D.C.
3. Springenschmid, R., Breitenbucher, R., and Mangold, M., "Development of the Cracking Frame and the Temperature-Stress Testing Machine," Proceeding of the International RILEM Symposium on Thermal Cracking in Concrete at Early Ages, Edited by R. Springenschmid, E & EF Spon, London, 1995.
4. Suh, Y.C., Hankins, K. & McCullough, B.F. (1992) "Early-Age Behavior of Continuously Reinforced Concrete Pavement and Calibration of the Failure Prediction Model in the CRCP-7 Program," Research Report 1244-3. Center for Transportation Research, The University of Texas at Austin, Austin, Texas.
5. Nam, J.H. (2005) "Early-Age Behavior of CRCP and Its Implications for Long-Term Performance," Ph.D. Dissertation, The University of Texas at Austin, Austin, Texas.
6. Kohler, E.R. (2005) "Experimental Mechanics of Crack Width in Full-Scale Sections of Continuously Reinforced Concrete Pavements," Ph.D. Dissertation, University of Illinois, Urbana Champaign, Illinois.
7. Zollinger, D.G., and E.J. Barenberg, "Continuously Reinforced Pavements: Punchouts and Other Distresses and Implications for Design," *Project IHR - 518, Illinois Cooperative Highway Research Program*, University of Illinois at Urbana-Champaign, March 1990.
8. LaCourseiere, S.A., M.I. Darter, and S.A. Smiley, "Structural Distress Mechanisms in Continuously Reinforced Concrete Pavement," *Transportation Engineering Series No. 20*, University of Illinois at Urbana-Champaign, 1978.
9. "Pavement Management Information System—Rater's Manual," Texas Department of Transportation, Austin Texas, 2004.